On statistical strain and stress energy bounds from homogenization and virtual testing

S. Saroukhani [a], R. Vafadari [b], R. Andersson [c], F. Larsson [c, *], K. Runesson [c]

[a] Dept. of Civil and Environmental Engineering, Cornell University, USA
[b] Dept. of Science and Engineering, Ghent University, Belgium
[c] Dept. of Applied Mechanics, Chalmers Univ. of Technology, Sweden

A B S T R A C T

Computational homogenization for quasistatic stress problems is considered, whereby the macroscale stress is obtained via averaging on Statistical Volume Elements (SVE:s). The variational "workhorse" for the subscale problem is derived from the presumption of weak micro-periodicity, which was proposed by Larsson et al. (2011). Continuum (visco)plasticity is adopted for the mesoscale constituents, whereby a pseudo-elastic, incremental strain energy serves as the potential for the updated stress in a given time-increment. Strict bounds on the incremental strain energy are derived from imposing Dirichlet and Neumann boundary conditions, which are defined as suitable restrictions of the proposed variational format. For this purpose, both the standard situation of complete macroscale strain control and the (less standard) situation of macroscale stress control are considered. Numerical results are obtained from "virtual testing" of SVE:s in terms of mean values and a given confidence interval, and it is shown how these properties converge with respect to the SVE-size for different prescribed macroscale deformation modes and different statistical properties of the random microstructure. In addition, the upper and lower bounds for a sequence of increasing strain levels, for a fixed SVE-size, are used as "data" for the calibration of a macroscopic elastic—plastic constitutive model.

1. Introduction

The standard approach to account for the effect of randomized material micro-heterogeneities in constitutive modeling is to employ fully "nested" macro-subscale modeling based on homogenization on a Statistical Volume Element[1] (SVE), (c.f. Michel et al., 1999; Miehe et al., 1999; Miehe and Koch, 2002; Torquato, 2002; Ostoja-Starzewski, 2006, 2008; Kouznetsova et al., 2002; Geers et al., 2010; Zohdi and Wriggers, 2001, 2005; Temizer and Wriggers, 2008; Roters et al., 2010; Schröder et al., 2011; Danielsson et al., 2007). Although the basic procedure is now quite well established, many issues are still unresolved, for example in relation to the model assumptions that are (implicitly and explicitly) made as part of the computation. Among the issues are (1) to formulate and

analytically assess the effectiveness of different prolongation conditions to the subscale (within the SVE) and to (2) establish rigorous bounds on energetic measures based on "virtual testing" of randomly chosen "samples" of the microstructural arrangement.

As to the first issue, it is clear that different model assumptions are possible in terms of the imposed boundary conditions and the appropriate variational format of the SVE-problem. The classical conditions are those of zero displacement fluctuation field (Dirichlet), boundary tractions generated by a constant macroscale stress tensor (Neumann) and (strong) micro-periodicity, defined by periodic displacement fluctuations and anti-periodic tractions. There is ample numerical evidence that periodic boundary conditions are efficient even when the microstructure is non-periodic (which is the most common situation). By "efficient" we here denote the property that the results converge rapidly when the SVE-size is increased (while the length-scale of the subscale features is kept fixed). However, it can not be generally proved for an arbitrary type of nonlinear and dissipative subscale constitutive assumption that the choice of periodic boundary conditions give the "best" results for a given size of the subscale computational domain on which the SVE-problem is defined. In this paper, we use

---

* Corresponding author.
E-mail address: fredrik.larsson@chalmers.se (F. Larsson).
[1] We prefer the notion SVE rather than the commonly used Representative Volume Element (RVE) since the fact that SVE:s of finite size are not truly representative is the topic of this paper.

a recently proposed weak form of micro-periodicity condition as a "work-horse" (Larsson et al., 2011). This format has a number of properties that are believed to be advantageous. For example, this format encompasses in a quite direct fashion (1) the classical "strong format" of micro-periodicity and (2) the Neumann boundary condition on tractions. As it turns out, the Neumann boundary condition is completely equivalent to the weakest possible form of displacement micro-periodicity. Moreover, (3) the Dirichlet boundary condition can also be obtained from this variational format by restricting the space of displacements in a suitable way. The resulting formulation is, however, "non-conventional" from an operational point of view (as discussed below).

As to the second issue (which is the main focus in this paper), it is first noted that a wealth of literature has been devoted to the issue of providing upper and lower bounds to the expected value of the effective stiffness in elasticity. Examples are Teply and Dvorak (1988), Huet (1990), Hazanov and Huet (1995), Suquet (1993), Suquet (1977), Zohdi and Wriggers (2001, 2005), Ostoja-Starzewski (2008), Salmi et al. (2012) and Brisard et al. (2013). However, the expected value is never computable in practice; only the mean values are. Therefore, the main contribution in this paper regards the procedure and strategy to achieve both upper and lower bounds with a given confidence based on computations for a given SVE-size. This task turns out to not be entirely trivial, particularly not for nonlinear and dissipative material models (such as elasto-plasticity).

The paper is organized as follows: After giving a summary of the essential assumptions and the variational framework for (first order) computational homogenization in Sections 2 and 3, we outline the SVE-problem pertinent to the proposed variational micro-periodicity condition for macroscale strain and stress control in Section 4. The main part is Section 5, which deals with energetic bounds based on statistical considerations. Finally, in Section 6 we illustrate the ideas with the aid of a few numerical examples on SVE-computations. The paper is concluded by final remarks and an outlook to future work.

2. Homogenization of quasistatic stress problem

2.1. Preliminaries

Consider the spatial domain Ω with boundary Γ. The usual continuum relations are assumed to apply on the subscale such that the equilibrium equation representing quasi-static response reads.

$$-\boldsymbol{\sigma} \cdot \boldsymbol{\nabla} = \boldsymbol{f} \quad \text{in } \Omega, \tag{1}$$

where $\boldsymbol{\sigma}$ is the stress, $\boldsymbol{\nabla}$ is the spatial gradient with respect to co-ordinates $\boldsymbol{x} \in \Omega$, and $\boldsymbol{f}$ is the body force. As to the relevant boundary conditions on Γ, we have the usual Neumann condition $\boldsymbol{t} \overset{\text{def}}{=} \boldsymbol{\sigma} \cdot \boldsymbol{n} = \boldsymbol{t}_{\text{p}}$ on Γ_{N}, where $\boldsymbol{n}$ is a unit normal vector, and the Dirichlet condition $u = \boldsymbol{u}_{\text{p}}$ on Γ_{D}. In order to simplify the subsequent discussion on homogenized properties and avoid unnecessary technical details, we shall henceforth assume that $\boldsymbol{t}_{\text{p}} = \boldsymbol{0}$.

Constitutive relations are needed to determine $\boldsymbol{\sigma}$ in terms of the (subscale) strain $\boldsymbol{\varepsilon}[\boldsymbol{u}] \overset{\text{def}}{=} (\boldsymbol{u} \otimes \boldsymbol{\nabla})^{\text{sym}}$ and, possibly, a set of internal variables $\underline{k}$ expressing dissipative mechanisms such that $\boldsymbol{\sigma}(\boldsymbol{\varepsilon}, \underline{k})$. Upon integrating the corresponding evolution equations in time and solving for $\underline{k}$ for given $\boldsymbol{\varepsilon}$, we obtain the *algorithmic* stress-deformation relation. $\boldsymbol{\sigma}_{\text{a}}(\boldsymbol{\varepsilon}) \overset{\text{def}}{=} \boldsymbol{\sigma}(\boldsymbol{\varepsilon}, \underline{k}_{\text{a}}(\boldsymbol{\varepsilon}))$[2] Note that any algorithmic variable is an implicit function of its argument; however, this fact is

not stressed further. The relation is explicit only if the material response is elastic.

Due to the excessive effort in resolving the fine scale representation, homogenization is introduced. The classical approach (which is adopted in this paper) is to introduce "model-based homogenization", whereby a local field y is replaced by the "running" volume average:

$$y(\overline{\boldsymbol{x}}) \mapsto \langle y \rangle_{\square}(\overline{\boldsymbol{x}}) \overset{\text{def}}{=} \frac{1}{|\Omega_{\square}(\overline{\boldsymbol{x}})|} \int_{\Omega_{\square}} y \, dV, \quad \overline{\boldsymbol{x}} \in \Omega \tag{2}$$

representing a smoothing approximation on a Statistical Volume Element (SVE). In practice, the SVE:s are finite-sized and occupies the subscale region $\Omega_{\square}(\overline{\boldsymbol{x}})$ with boundary $\Gamma_{\square}$.[3] The typical dimension of an SVE is $L_{\square} = (|\Omega_{\square}|)^{1/n_{\text{dim}}}$, where $n_{\text{dim}} \in \{1, 2, 3\}$ is the spatial dimension. The SVE is centered at the macroscale position[4] $\overline{\boldsymbol{x}} \overset{\text{def}}{=} (1/|\Omega_{\square}|) \int \boldsymbol{x} \, dS$ for any given $\overline{\boldsymbol{x}} \in \Omega$.

In order to establish the homogenized version of the weak format of equilibrium, we introduce the space-variational forms.

$$a(\boldsymbol{u}; \delta\boldsymbol{u}) \overset{\text{def}}{=} \int_{\Omega} \langle \boldsymbol{\sigma}(\boldsymbol{\varepsilon}[\boldsymbol{u}]) : \boldsymbol{\varepsilon}[\delta\boldsymbol{u}] \rangle_{\square} \, dV, \quad l(\delta\boldsymbol{u}) \overset{\text{def}}{=} \int_{\Omega} \langle \boldsymbol{f} \cdot \delta\boldsymbol{u} \rangle_{\square} \, dV \tag{3}$$

representing the internal and external virtual work, respectively, of the homogenized problem. The appropriate homogenized virtual work relation is thus given as: Find $\boldsymbol{u} \in \mathbb{U}$ s.t.

$$a(\boldsymbol{u}; \delta\boldsymbol{u}) = l(\delta\boldsymbol{u}), \quad \forall \delta\boldsymbol{u} \in \mathbb{U}^0 \tag{4}$$

Inside each SVE, the subscale displacement field is split into one smooth part, $\boldsymbol{u}^{\text{M}}$, and the subscale fluctuation, $\boldsymbol{u}^{\text{s}}$, i.e. $\boldsymbol{u} = \boldsymbol{u}^{\text{M}} + \boldsymbol{u}^{\text{s}}$. The scales are linked by expressing $\boldsymbol{u}^{\text{M}}(\overline{\boldsymbol{x}}, \boldsymbol{x})$[5] for $\overline{\boldsymbol{x}} \in \Omega$ and $\boldsymbol{x} \in \Omega_{\square}(\overline{\boldsymbol{x}})$ in terms of the macroscale solution $\overline{\boldsymbol{u}}(\overline{\boldsymbol{x}})$ in an explicit fashion and defining the *approximate* solution $\boldsymbol{u}^{\text{s}} = \boldsymbol{u}^{\text{s}}\{\overline{\boldsymbol{u}}\}$[6] for given $\overline{\boldsymbol{u}}$. This (implicit) relation allows for computing the homogenized quantities in (3). Moreover, we introduce the standard assumption on (model-based) *first order homogenization*, according to which the macroscale field $\boldsymbol{u}^{\text{M}}$ varies *linearly* within each SVE. This means that we expand $\boldsymbol{u}^{\text{M}}$ as.

$$\boldsymbol{u}^{\text{M}}(\overline{\boldsymbol{x}}, \boldsymbol{x}) = \overline{\boldsymbol{u}}(\overline{\boldsymbol{x}}) + \overline{\boldsymbol{\varepsilon}}(\overline{\boldsymbol{x}}) \cdot [\boldsymbol{x} - \overline{\boldsymbol{x}}], \quad \overline{\boldsymbol{x}} \in \Omega, \quad \boldsymbol{x} \in \Omega_{\square}(\overline{\boldsymbol{x}}). \tag{5}$$

Here we introduced the (smooth) macroscopic displacement field $\overline{\boldsymbol{u}}$ and the corresponding strain field $\overline{\boldsymbol{\varepsilon}} \overset{\text{def}}{=} (\overline{\boldsymbol{u}} \otimes \boldsymbol{\nabla})^{\text{sym}} = \boldsymbol{\varepsilon}[\overline{\boldsymbol{u}}]$.

It is now tacitly used that the variation $\delta\boldsymbol{u}$ can be defined as the sensitivity[7] for a variation $\delta\overline{\boldsymbol{u}}$ and thus can be expressed as $\delta\boldsymbol{u} = \delta\boldsymbol{u}^{\text{M}} + (\boldsymbol{u}^{\text{s}})'\{\overline{\boldsymbol{u}}; \delta\overline{\boldsymbol{u}}\}$, where

$$\delta\boldsymbol{u}^{\text{M}} = \delta\overline{\boldsymbol{u}} + \delta\overline{\boldsymbol{\varepsilon}} \cdot [\boldsymbol{x} - \overline{\boldsymbol{x}}] \tag{6}$$

Upon setting $\delta\boldsymbol{u} = \delta\boldsymbol{u}^{\text{M}}$ in (4), we obtain the macroscopic problem as that of finding $\overline{\boldsymbol{u}} \in \overline{\mathbb{U}}$ that solves the homogenized problem.

$$a(\boldsymbol{u}\{\overline{\boldsymbol{u}}\}; \delta\boldsymbol{u}^{\text{M}}(\delta\overline{\boldsymbol{u}})) = l(\delta\boldsymbol{u}^{\text{M}}(\delta\overline{\boldsymbol{u}})) \quad \forall \delta\overline{\boldsymbol{u}} \in \overline{\mathbb{U}}^0. \tag{7}$$

---

[2] Henceforth, the subindex "a" is dropped without the risk of confusion.

[3] Henceforth, the argument $\overline{\boldsymbol{x}}$ is suppressed unless there is a risk of confusion.

[4] The choice is not unique: Another possibility is $\overline{\boldsymbol{x}} = \langle \boldsymbol{x} \rangle_{\square}$.

[5] Double arguments, e.g. $\boldsymbol{u}(\overline{\boldsymbol{x}}, \boldsymbol{x})$, are used to explicitly point out the underlying scale separation.

[6] Curly brackets $\{(\bullet)\}$ indicate implicit and/or nonlocal functional dependence on $(\bullet)$.

[7] The sensitivity is defined as the Gateaux-derivative $(\boldsymbol{u}^{\text{s}})'\{\overline{\boldsymbol{u}}; \delta\overline{\boldsymbol{u}}\} \overset{\text{def}}{=} (\partial/\partial\varepsilon) \boldsymbol{u}^{\text{s}}\{\overline{\boldsymbol{u}} + \varepsilon\delta\overline{\boldsymbol{u}}\}|_{\varepsilon=0}$.

More explicitly, (7) can be expressed as the problem of finding $\overline{\boldsymbol{u}} \in \overline{\mathbb{U}}$ that solves.

$$\int_{\Omega} \overline{\boldsymbol{\sigma}}\{\overline{\boldsymbol{\varepsilon}}\} : \boldsymbol{\varepsilon}[\delta\overline{\boldsymbol{u}}] \, \mathrm{d}V = \int_{\Omega} [\overline{\boldsymbol{f}} \cdot \delta\overline{\boldsymbol{u}} + \overline{\boldsymbol{f}}^{(2)} : \boldsymbol{\varepsilon}[\delta\overline{\boldsymbol{u}}]] \mathrm{d}V \quad \forall \delta\overline{\boldsymbol{u}} \in \overline{\mathbb{U}}^0 \qquad (8)$$

with the following auxiliary definitions of the macroscale variables

$$\overline{\boldsymbol{\sigma}} \stackrel{\mathrm{def}}{=} \langle \boldsymbol{\sigma} \rangle_{\square}, \ \overline{\boldsymbol{f}} \stackrel{\mathrm{def}}{=} \langle \boldsymbol{f} \rangle_{\square}, \ \overline{\boldsymbol{f}}^{(2)} \stackrel{\mathrm{def}}{=} \langle \boldsymbol{f} \otimes [\boldsymbol{x} - \overline{\boldsymbol{x}}] \rangle_{\square} \qquad (9)$$

Remark: In order for (7) to be a valid expression of homogenization, a generalized form of the Hill–Mandel condition should hold, e.g. Larsson et al. (2010). It is satisfied for the standard choice of boundary conditions (Dirichlet, Neumann, Strongly Periodic) as well the novel Weakly Periodic boundary conditions that are exploited in the next Section.

2.2. Canonical format of the SVE-problem

To avoid unnecessary technical complexity without obscuring the main ideas, we shall henceforth consider the case without volume force, i.e. $\boldsymbol{f} = \boldsymbol{0}$. The quasi-static subscale (local) moment balance on a given SVE is then stated in the most general format as.

$$a_{\square}(\boldsymbol{u}; \delta\boldsymbol{u}) - \frac{1}{|\Omega_{\square}|} \int_{\Gamma_{\square}} \boldsymbol{t} \cdot \delta\boldsymbol{u} \, \mathrm{d}S = 0 \qquad (10)$$

where

$$a_{\square}(\boldsymbol{u}; \delta\boldsymbol{u}) \stackrel{\mathrm{def}}{=} \langle \boldsymbol{\sigma}(\boldsymbol{\varepsilon}) : \boldsymbol{\varepsilon}[\delta\boldsymbol{u}] \rangle_{\square} \qquad (11)$$

Further, we shall require that the following auxiliary identities/conditions be satisfied:

$$\overline{\boldsymbol{\sigma}} : \delta\overline{\boldsymbol{\varepsilon}} = \langle \boldsymbol{\sigma} \rangle_{\square} : \delta\overline{\boldsymbol{\varepsilon}} \quad \forall \delta\overline{\boldsymbol{\varepsilon}} \in \mathbb{R}^{3\times3}_{\mathrm{sym}} \qquad (12)$$

$$\overline{\boldsymbol{\varepsilon}} : \delta\overline{\boldsymbol{\sigma}} = \langle \boldsymbol{\varepsilon} \rangle_{\square} : \delta\overline{\boldsymbol{\sigma}} \quad \forall \delta\overline{\boldsymbol{\sigma}} \in \mathbb{R}^{3\times3}_{\mathrm{sym}} \qquad (13)$$
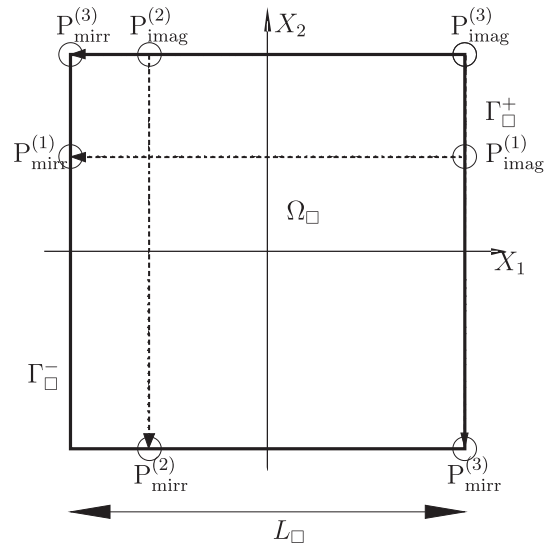
We note the (very useful) representations.

$$\langle \boldsymbol{\sigma} \rangle_{\square} = \frac{1}{|\Omega_{\square}|} \int_{\Gamma_{\square}} (\boldsymbol{t} \otimes [\boldsymbol{x} - \overline{\boldsymbol{x}}])^{\mathrm{sym}} \, \mathrm{d}S,$$

$$\langle \boldsymbol{\varepsilon} \rangle_{\square} = \frac{1}{|\Omega_{\square}|} \int_{\Gamma_{\square}} (\boldsymbol{u} \otimes \boldsymbol{n})^{\mathrm{sym}} \, \mathrm{d}S \qquad (14)$$

Two situations now arise as to the "loading" of the SVE:

- In the (standard) case of complete macroscale strain control, $\overline{\boldsymbol{\varepsilon}}$ is a known quantity at the solution of the SVE-problem, whereby (10) is complemented with the condition (13). In a post-processing step, $\overline{\boldsymbol{\sigma}}$ is computed from (12).
- In the (non-standard) case of complete macroscale stress control, $\overline{\boldsymbol{\sigma}}$ is a known quantity at the solution of the SVE-problem, whereby (10) is complemented with the condition (12). In a post-processing step, $\overline{\boldsymbol{\varepsilon}}$ is computed from (13).

The SVE-problem (10) is not uniquely solvable without further modeling assumptions (restrictions) on the variation of $\boldsymbol{u}$ or $\boldsymbol{t}$. In this paper we adopt a recently proposed variational framework allowing for weak satisfaction of micro-periodicity, cf. Larsson et al. (2011), and this framework will be briefly summarized in what follows.

Fig. 1. SVE in 2D with "image" and "mirror" boundaries. Note that the corner point $P^{(3)}_{\mathrm{imag}}$ has two mirror points (corners).

We assume that the subscale fluctuation field $\boldsymbol{u}^{\mathrm{s}}$ is periodic across the SVE boundaries w.r.t. the chosen local coordinate axes. This model assumption on "micro-periodicity" is a key ingredient (and frequently adopted) in the literature on mathematical homogenization and can be viewed as an approximation between the stiffer Dirichlet and the weaker Neumann boundary conditions. Indeed, both these cases can be obtained as special cases of the most general variational format of periodicity (as will be discussed further below).

In order to formulate the conditions on micro-periodicity, we consider the SVE in Fig. 1, where the boundary $\Gamma_{\square}$ has been split into two parts: $\Gamma_{\square} = \Gamma_{\square}^{-} \cup \Gamma_{\square}^{+}$. Here, $\Gamma_{\square}^{+}$ is the *image boundary* (later chosen as the computational domain for boundary integration), whereas Γ^{-} is the *mirror boundary*. We shall now introduce the proper mapping $\boldsymbol{\varphi}_{\mathrm{per}}: \Gamma^{+} \rightarrow \Gamma^{-}$ such that any point $\boldsymbol{x}^{+} \in \Gamma_{\square}^{+}$ is mirrored in a self-similar fashion to the corresponding point $\boldsymbol{x}^{-} \in \Gamma_{\square}^{-}$; hence, $\boldsymbol{x}^{-} = \boldsymbol{\varphi}_{\mathrm{per}}(\boldsymbol{x}^{+})$.[8]

In particular, we express micro-periodicity of the displacement fluctuation field as.

$$\boldsymbol{u}^{\mathrm{s}}(\boldsymbol{x}) = \boldsymbol{u}^{\mathrm{s}}(\boldsymbol{\varphi}_{\mathrm{per}}(\boldsymbol{x})), \quad \forall \boldsymbol{x} \in \Gamma_{\square}^{+} \qquad (15)$$

or, equivalently, in terms of the "jump" between the fluctuation fields on the image and mirror parts of the boundary as follows:

$$[\![\boldsymbol{u}^{\mathrm{s}}]\!] = \boldsymbol{0} \quad \text{on } \Gamma_{\square}^{+}, \quad [\![\boldsymbol{u}^{\mathrm{s}}]\!](\boldsymbol{x}) \stackrel{\mathrm{def}}{=} \boldsymbol{u}^{\mathrm{s}}(\boldsymbol{x}) - \boldsymbol{u}^{\mathrm{s}}(\boldsymbol{\varphi}_{\mathrm{per}}(\boldsymbol{x})), \quad \forall \boldsymbol{x} \in \Gamma_{\square}^{+} \qquad (16)$$

Subsequently, we shall not enforce the condition (16) strongly as the point of departure; rather it is done weakly. To this end, we assume that the boundary tractions $\boldsymbol{t} \stackrel{\mathrm{def}}{=} \boldsymbol{\sigma} \cdot \boldsymbol{n}$ satisfy the *anti-symmetry condition* for any regular mirror point.

$$\boldsymbol{t}(\boldsymbol{x}) = -\boldsymbol{t}(\boldsymbol{\varphi}_{\mathrm{per}}(\boldsymbol{x})), \quad \forall \boldsymbol{x} \in \Gamma_{\square}^{+} \qquad (17)$$

as depicted in Fig. 1, and it is noted that $\boldsymbol{t} \in \mathbb{T}_{\square}$.

We now evaluate, upon using (17), the boundary term in (10) as follows:

---

[8] There is a unique mirror point for each $\boldsymbol{x}^{+} \in \Gamma_{\square}^{+}$ except for points on edges (in 3D) and in corners (in 2D, 3D).

$$\int_{\Gamma_\square} \boldsymbol{t} \cdot \delta\boldsymbol{u} \, \mathrm{d}S = \int_{\Gamma_\square^+} \boldsymbol{t} \cdot [\![\delta\boldsymbol{u}]\!] \, \mathrm{d}S \tag{18}$$

A variational (weak) statement of the micro-periodicity constraint already given in (16) can be given as.

$$d_\square(\delta\boldsymbol{t}, \boldsymbol{u}^s) \overset{\mathrm{def}}{=} \frac{1}{|\Omega_\square|} \int_{\Gamma_\square^+} \delta\boldsymbol{t} \cdot [\![\boldsymbol{u}^s]\!] \, \mathrm{d}S = 0, \quad \forall \delta\boldsymbol{t} \in \mathbb{T}_\square^+ \tag{19}$$

where $\mathbb{T}_\square^+$ is the trace of functions in $\mathbb{T}_\square$[9] on the image boundary $\Gamma_\square^+$. Hence, all tractions of any concern live on $\Gamma_\square^+$ only.

Next, we consider the two situations of macrostrain and macrostress control in turn.

2.3. Macroscale strain control

Based on the developments in the previous Subsection, the variational form of the subscale problem for weakly imposed microperiodicity in the displacements can now be formulated for the case of macrostrain control as follows: Find $\boldsymbol{u} \in \mathbb{U}_\square$ and $\boldsymbol{t} \in \mathbb{T}_\square$ that, for given value of the macroscale displacement gradient $\bar{\boldsymbol{\varepsilon}}$, solve the system.

$$\begin{aligned} a_\square(\boldsymbol{u}; \delta\boldsymbol{u}) - d_\square(\boldsymbol{t}, \delta\boldsymbol{u}) &= 0 & \forall \delta\boldsymbol{u} \in \mathbb{U}_\square, \\ -d_\square(\delta\boldsymbol{t}, \boldsymbol{u}) &= -d_\square(\delta\boldsymbol{t}, \bar{\boldsymbol{\varepsilon}} \cdot [\boldsymbol{x} - \bar{\boldsymbol{x}}]) & \forall \delta\boldsymbol{t} \in \mathbb{T}_\square. \end{aligned} \tag{20}$$

It is noted that $(20)_2$ represents a trivial reformulation of the variational micro-periodicity condition in (19) when the assumed linear variation in (5) is used. As to the iterative solution of the system (20), Newton's method for finding $\boldsymbol{u}$ and $\boldsymbol{t}$ is conveniently used.

It is possible to identify the problem defined by Dirichlet boundary conditions from the general format upon restricting the space $\mathbb{U}_\square$, i.e. introducing $\mathbb{U}_\square^D \subseteq \mathbb{U}_\square$ defined as.

$$\mathbb{U}_\square^D = \{\boldsymbol{u} \in \mathbb{U}_\square : \exists \widehat{\bar{\boldsymbol{\varepsilon}}} \in \mathbb{R}_{\mathrm{sym}}^{3\times3} \text{ s.t. } \boldsymbol{u} = \widehat{\bar{\boldsymbol{\varepsilon}}} \cdot [\boldsymbol{x} - \bar{\boldsymbol{x}}] \text{ on } \Gamma_\square\} \tag{21}$$

while $\mathbb{T}_\square^D = \mathbb{T}_\square$ is left unrestricted. The pertinent solution is now obtained from (20). In fact, the usual "operational format" that admits easy FE-implementation can be derived from (20) as follows: Eq. $(20)_2$ gives, with the definition in (19), the equation

$$[\widehat{\bar{\boldsymbol{\varepsilon}}} - \bar{\boldsymbol{\varepsilon}}] : \frac{1}{|\Omega_\square|} \int_{\Gamma_\square^+} \delta\boldsymbol{t} \otimes [\![\boldsymbol{x}]\!] \, \mathrm{d}S = 0 \quad \forall \delta\boldsymbol{t} \in \mathbb{T}_\square \tag{22}$$

Choosing $\delta\boldsymbol{t} = \delta\widehat{\boldsymbol{\sigma}} \cdot \boldsymbol{n}$, with $\delta\widehat{\boldsymbol{\sigma}} \in \mathbb{R}_{\mathrm{sym}}^{3\times3}$, we conclude that $\widehat{\bar{\boldsymbol{\varepsilon}}} = \bar{\boldsymbol{\varepsilon}}$ is the (given) value that defines the functions in $\mathbb{U}_\square^D$. Taking advantage of this fact, we may introduce the space.

$$\mathbb{U}_\square^D(\bar{\boldsymbol{\varepsilon}}) = \{\boldsymbol{u} \in \mathbb{U}_\square : \boldsymbol{u} = \bar{\boldsymbol{\varepsilon}} \cdot [\boldsymbol{x} - \bar{\boldsymbol{x}}] \text{ on } \Gamma_\square\} \tag{23}$$

and the corresponding space of test functions is $\mathbb{U}_\square^D(\boldsymbol{0})$. Now, it is clear that $d_\square(\boldsymbol{t}, \delta\boldsymbol{u}) = 0, \quad \forall \delta\boldsymbol{u} \in \mathbb{U}_\square^D(\boldsymbol{0})$. The operational (standard) format then becomes: For given value of $\bar{\boldsymbol{\varepsilon}} \in \mathbb{R}_{\mathrm{sym}}^{3\times3}$, find $\boldsymbol{u} \in \mathbb{U}_\square^D(\bar{\boldsymbol{\varepsilon}})$ that solves

$$a_\square(\boldsymbol{u}; \delta\boldsymbol{u}) = 0 \quad \forall \delta\boldsymbol{u} \in \mathbb{U}_\square^D(\boldsymbol{0}). \tag{24}$$

When the solution has been found it is possible to compute $\bar{\boldsymbol{\sigma}}$ in a "post-processing step": $\bar{\boldsymbol{\sigma}} = \langle\boldsymbol{\sigma}\rangle_\square$.

---

[9] Henceforth we drop superscript "+" and use the simpler notation $\mathbb{T}_\square$.

The problem defined by Neumann boundary conditions is obtained from the general format (20) upon restricting the space $\mathbb{T}_\square$, i.e. introducing $\mathbb{T}_\square^N \subseteq \mathbb{T}_\square$ defined as.

$$\mathbb{T}_\square^N = \{\boldsymbol{t} \in \mathbb{T}_\square : \exists \widehat{\bar{\boldsymbol{\sigma}}} \in \mathbb{R}_{\mathrm{sym}}^{3\times3} \text{ s.t. } \boldsymbol{t} = \widehat{\bar{\boldsymbol{\sigma}}} \cdot \boldsymbol{n} \text{ on } \Gamma_\square\} \tag{25}$$

while $\mathbb{U}_\square^N = \mathbb{U}_\square$ is left unrestricted. Clearly, this space restricts the tractions to become piecewise constant on each of the three positive boundary faces of the SVE-cube. The pertinent solution is, again, obtained from (20). The corresponding operational format, that admits easy FE-implementation, can be derived from (20) as follows:

$$\begin{aligned} a_\square(\boldsymbol{u}; \delta\boldsymbol{u}) - d_\square(\bar{\boldsymbol{\sigma}} \cdot \boldsymbol{n}, \delta\boldsymbol{u}) &= 0 & \forall \delta\boldsymbol{u} \in \mathbb{U}_\square, \\ -c_\square(\delta\bar{\boldsymbol{\sigma}} \cdot \boldsymbol{n}, \boldsymbol{u}) &= -\delta\bar{\boldsymbol{\sigma}} : \bar{\boldsymbol{\varepsilon}} & \forall \delta\bar{\boldsymbol{\sigma}} \in \mathbb{R}_{\mathrm{sym}}^{3\times3}. \end{aligned} \tag{26}$$

Remark: The Neumann condition represents the weakest possible way of enforcing the micro-periodicity condition. Here it is considered as a *model assumption*; however, it is also possible to view this choice as a (crude) FE-approximation of the traction field.

2.4. Macroscale stress control

All numerical results in this paper are obtained using macroscale strain control. However, for completeness and to provide the basis for bounds on the complementary energy in terms of macroscale stresses (as discussed below), we also present the variational forms that are pertinent to macroscale stress control. The unified variational form of the subscale problem in such a case can be formulated as follows: Find $\boldsymbol{u} \in \mathbb{U}_\square$, $\boldsymbol{t} \in \mathbb{T}_\square$ and $\bar{\boldsymbol{\varepsilon}} \in \mathbb{R}_{\mathrm{sym}}^{3\times3}$ that, for given value of the macroscale stress $\bar{\boldsymbol{\sigma}}$, solve the system.

$$\begin{aligned} a_\square(\boldsymbol{u}; \delta\boldsymbol{u}) - d_\square(\boldsymbol{t}, \delta\boldsymbol{u}) &= 0 & \forall \delta\boldsymbol{u} \in \mathbb{U}_\square, \\ -d_\square(\delta\boldsymbol{t}, \boldsymbol{u}) + d_\square(\delta\boldsymbol{t}, \bar{\boldsymbol{\varepsilon}} \cdot [\boldsymbol{x} - \bar{\boldsymbol{x}}]) &= 0 & \forall \delta\boldsymbol{t} \in \mathbb{T}_\square \\ d_\square(\boldsymbol{t}, \delta\bar{\boldsymbol{\varepsilon}} \cdot [\boldsymbol{x} - \bar{\boldsymbol{x}}]) &= \bar{\boldsymbol{\sigma}} : \delta\bar{\boldsymbol{\varepsilon}} & \forall \delta\bar{\boldsymbol{\varepsilon}} \in \mathbb{R}_{\mathrm{sym}}^{3\times3} \end{aligned} \tag{27}$$

Like in the case of macroscale strain control, it is possible to identify the problem defined by Dirichlet boundary conditions from the unified format in (27) upon introducing the space $\mathbb{U}_\square^D \subseteq \mathbb{U}_\square$, which is defined in (21), while $\mathbb{T}_\square^D = \mathbb{T}_\square$ is left unrestricted. Even in this case we obtain from $(27)_2$ that $\widehat{\bar{\boldsymbol{\varepsilon}}} = \bar{\boldsymbol{\varepsilon}}$ and the space $\mathbb{U}_\square^D(\bar{\boldsymbol{\varepsilon}})$ in (23) is utilized. Moreover, combining the result in $(27)_3$ with $(27)_1$, we obtain.

$$a_\square(\boldsymbol{u}; \delta\boldsymbol{u}) = 0 \quad \forall \delta\boldsymbol{u} \in \mathbb{U}_\square^D \tag{28}$$

Upon introducing the split $\boldsymbol{u} = \boldsymbol{u}^M + \boldsymbol{u}^s$, where $\boldsymbol{u}^M(\bar{\boldsymbol{\varepsilon}}) = \bar{\boldsymbol{\varepsilon}} \cdot [\boldsymbol{x} - \bar{\boldsymbol{x}}] \in \mathbb{U}_\square^D(\bar{\boldsymbol{\varepsilon}})$ and $\boldsymbol{u}^s \in \mathbb{U}_\square^D(\boldsymbol{0})$, we obtain from (28) the SVE-problem: For given value of the macroscale stress $\bar{\boldsymbol{\sigma}} \in \mathbb{R}_{\mathrm{sym}}^{3\times3}$, find $\boldsymbol{u}^s \in \mathbb{U}_\square^{D,s}$ and $\bar{\boldsymbol{\varepsilon}} \in \mathbb{R}_{\mathrm{sym}}^{3\times3}$ that solve.

$$\begin{aligned} a_\square(\boldsymbol{u}^M(\bar{\boldsymbol{\varepsilon}}) + \boldsymbol{u}^s; \delta\boldsymbol{u}^s) &= 0 & \forall \delta\boldsymbol{u}^s \in \mathbb{U}_\square^D(\boldsymbol{0}) \\ \langle\boldsymbol{\sigma}(\boldsymbol{\varepsilon}[\boldsymbol{u}^M(\bar{\boldsymbol{\varepsilon}}) + \boldsymbol{u}^s])\rangle_\square : \delta\bar{\boldsymbol{\varepsilon}} &= \bar{\boldsymbol{\sigma}} : \delta\bar{\boldsymbol{\varepsilon}} & \forall \delta\bar{\boldsymbol{\varepsilon}} \in \mathbb{R}_{\mathrm{sym}}^{3\times3} \end{aligned} \tag{29}$$

which is the proper operational format. We note that the test functions $\delta\boldsymbol{u}^s \in \mathbb{U}_\square^D(\boldsymbol{0})$ and $\delta\bar{\boldsymbol{\varepsilon}} \in \mathbb{R}^{3\times3}$ are chosen completely independently, and that the space of tractions, $\mathbb{U}_\square^D$, becomes irrelevant.

Again, like in the case of macroscale strain control, it is possible to identify the problem defined by Neumann boundary conditions from the unified format in (27) upon introducing the space $\mathbb{U}_\square^N = \mathbb{U}_\square$ while $\mathbb{T}_\square^N \subseteq \mathbb{T}_\square$ was defined in (25). In this case we obtain from $(27)_3$ that $\widehat{\bar{\boldsymbol{\sigma}}} = \bar{\boldsymbol{\sigma}}$. From $(27)_1$ we then obtain the following problem: For given value of $\bar{\boldsymbol{\sigma}} \in \mathbb{R}_{\mathrm{sym}}^{3\times3}$, find $\boldsymbol{u} \in \mathbb{U}_\square^N$ that solves.

$$a_\square(\boldsymbol{u};\delta\boldsymbol{u}) = \langle\boldsymbol{\varepsilon}[\delta\boldsymbol{u}]\rangle_\square : \overline{\boldsymbol{\sigma}} \quad \forall\delta\boldsymbol{u}\in\mathbb{U}_\square^N \tag{30}$$

When the solution has been found it is possible to compute $\overline{\boldsymbol{\varepsilon}}$ in a "post-processing step" from $(27)_2$: $\overline{\boldsymbol{\varepsilon}} = \langle\boldsymbol{\varepsilon}\rangle_\square$.

3. Energetic considerations and bounds for a single SVE-realization

3.1. Properties of macroscale strain and stress energies

We first consider macroscale strain control and assume from the outset that there exists a subscale (volume-specific) strain energy density[10] $w\{\boldsymbol{\varepsilon}\}$ such that $\boldsymbol{\sigma} = \mathrm{d}w\{\boldsymbol{\varepsilon}\}/\mathrm{d}\boldsymbol{\varepsilon}$. For a given realization of the micro-heterogenous material structure within the SVE of size $L_\square$ and subjected to micro-periodicity, the subscale gradient $\boldsymbol{\varepsilon}$ depends (implicitly) on $\overline{\boldsymbol{\varepsilon}}$ via the subscale field $\boldsymbol{u}\{\overline{\boldsymbol{\varepsilon}}\}$ that solves the pertinent SVE-problem; hence, $\boldsymbol{\varepsilon} = \boldsymbol{\varepsilon}[\boldsymbol{u}\{\overline{\boldsymbol{\varepsilon}}\}]$. We may then introduce the "incremental SVE-functional" $W_\square(\boldsymbol{u})$, for a given finite-sized SVE, as follows:

$$W_\square(\boldsymbol{u}) \overset{\mathrm{def}}{=} \langle w(\boldsymbol{\varepsilon}[\boldsymbol{u}])\rangle_\square \tag{31}$$

which is assumed to be convex in the continuous space $\mathbb{U}_\square$. A useful property is that the solution to the problem (20), for given $\overline{\boldsymbol{\varepsilon}}$, satisfies the min−max property

$$(\boldsymbol{u},\boldsymbol{t}) = \arg[\min_{\widehat{\boldsymbol{u}}\in\mathbb{U}_\square} \max_{\widehat{\boldsymbol{t}}\in\mathbb{T}_\square} \Pi_\square(\overline{\boldsymbol{\varepsilon}};\widehat{\boldsymbol{u}},\widehat{\boldsymbol{t}})] \tag{32}$$

where the Hellinger−Reissner type of functional $\Pi_\square(\overline{\boldsymbol{\varepsilon}};\widehat{\boldsymbol{u}},\widehat{\boldsymbol{t}})$ is defined as

$$\Pi_\square(\overline{\boldsymbol{\varepsilon}};\widehat{\boldsymbol{u}},\widehat{\boldsymbol{t}}) \overset{\mathrm{def}}{=} W_\square(\widehat{\boldsymbol{u}}) - d_\square(\widehat{\boldsymbol{t}},\widehat{\boldsymbol{u}}) - d_\square(\widehat{\boldsymbol{t}},-\overline{\boldsymbol{\varepsilon}}\cdot[\boldsymbol{x}-\overline{\boldsymbol{x}}]) \tag{33}$$

The saddle-point value is identical to the macroscale volume-specific incremental strain energy density $\overline{w}_\square\{\overline{\boldsymbol{\varepsilon}}\}$,

$$\begin{aligned}\overline{w}_\square\{\overline{\boldsymbol{\varepsilon}}\} &\overset{\mathrm{def}}{=} \inf_{\widehat{\boldsymbol{u}}\in\mathbb{U}_\square} \sup_{\widehat{\boldsymbol{t}}\in\mathbb{T}_\square} \Pi_\square(\overline{\boldsymbol{\varepsilon}};\widehat{\boldsymbol{u}},\widehat{\boldsymbol{t}}) \\ &= \Pi_\square(\overline{\boldsymbol{\varepsilon}};\boldsymbol{u}\{\overline{\boldsymbol{\varepsilon}}\},\boldsymbol{t}\{\overline{\boldsymbol{\varepsilon}}\}) = W_\square(\boldsymbol{u}\{\overline{\boldsymbol{\varepsilon}}\})\end{aligned} \tag{34}$$

where the last equality in (34) follows from $(20)_2$ upon choosing the test function $\delta\boldsymbol{t} = \boldsymbol{t}\{\overline{\boldsymbol{\varepsilon}}\}\in\mathbb{T}_\square$. As expected, $\overline{w}_\square\{\overline{\boldsymbol{\varepsilon}}\}$ is a potential for $\overline{\boldsymbol{\sigma}}$ in the classical sense, i.e. $\overline{\boldsymbol{\sigma}}$ can be obtained as

$$\overline{\boldsymbol{\sigma}}\{\overline{\boldsymbol{\varepsilon}}\} = \frac{\mathrm{d}\overline{w}_\square\{\overline{\boldsymbol{\varepsilon}}\}}{\mathrm{d}\overline{\boldsymbol{\varepsilon}}} \tag{35}$$

Moreover, it can be shown that the macroscale energy density $\overline{w}_\square\{\overline{\boldsymbol{\varepsilon}}\}$ is convex in the discrete space $\mathbb{R}_{\mathrm{sym}}^{3\times3}$, and we obtain the ATS-tensor $\overline{\mathsf{E}}_\square\{\overline{\boldsymbol{\varepsilon}}\}$ as the positive definite Hessian of $\overline{w}_\square\{\overline{\boldsymbol{\varepsilon}}\}$. An operational procedure for calculating $\overline{\mathsf{E}}_\square\{\overline{\boldsymbol{\varepsilon}}\}$ was given previously. Proofs of the various statements above are given in Appendix A.

Next, we consider macroscale stress control and note that the solution to the pertinent SVE-problem defined in (27), for given $\overline{\boldsymbol{\sigma}}$, satisfies.

$$(\boldsymbol{u},\boldsymbol{t},\overline{\boldsymbol{\varepsilon}}) = \arg[\max_{\widehat{\boldsymbol{u}}\in\mathbb{U}_\square} \min_{\widehat{\boldsymbol{t}}\in\mathbb{T}_\square} \max_{\widehat{\overline{\boldsymbol{\varepsilon}}}\in\mathbb{R}_{\mathrm{sym}}^{3\times3}} \Pi_\square^*(\overline{\boldsymbol{\sigma}};\widehat{\boldsymbol{u}},\widehat{\boldsymbol{t}},\widehat{\overline{\boldsymbol{\varepsilon}}})] \tag{36}$$

where the "complementary" Hellinger−Reissner type of functional $\Pi_\square^*(\overline{\boldsymbol{\sigma}};\widehat{\boldsymbol{u}},\widehat{\boldsymbol{t}},\widehat{\overline{\boldsymbol{\varepsilon}}})$ is defined as

$$\Pi_\square^*(\overline{\boldsymbol{\sigma}};\widehat{\boldsymbol{u}},\widehat{\boldsymbol{t}},\widehat{\overline{\boldsymbol{\varepsilon}}}) \overset{\mathrm{def}}{=} \overline{\boldsymbol{\sigma}} : \widehat{\overline{\boldsymbol{\varepsilon}}} - W_\square(\widehat{\boldsymbol{u}}) + d_\square(\widehat{\boldsymbol{t}},\widehat{\boldsymbol{u}}) - d_\square(\widehat{\boldsymbol{t}},\widehat{\overline{\boldsymbol{\varepsilon}}}\cdot[\boldsymbol{x}-\overline{\boldsymbol{x}}]) \tag{37}$$

The saddle-point value is identical to the stress (or complementary strain) volume-specific incremental energy density $\overline{w}_\square^*\{\overline{\boldsymbol{\sigma}}\}$,

$$\begin{aligned}\overline{w}_\square^*\{\overline{\boldsymbol{\sigma}}\} &\overset{\mathrm{def}}{=} \sup_{\widehat{\boldsymbol{u}}\in\mathbb{U}_\square} \inf_{\widehat{\boldsymbol{t}}\in\mathbb{T}_\square} \sup_{\widehat{\overline{\boldsymbol{\varepsilon}}}\in\mathbb{R}_{\mathrm{sym}}^{3\times3}} \Pi_\square^*(\overline{\boldsymbol{\sigma}};\widehat{\boldsymbol{u}},\widehat{\boldsymbol{t}},\widehat{\overline{\boldsymbol{\varepsilon}}}) \\ &= \Pi_\square^*(\overline{\boldsymbol{\sigma}};\boldsymbol{u}\{\overline{\boldsymbol{\sigma}}\},\boldsymbol{t}\{\overline{\boldsymbol{\sigma}}\},\overline{\boldsymbol{\varepsilon}}\{\overline{\boldsymbol{\sigma}}\}) = \overline{\boldsymbol{\sigma}} : \overline{\boldsymbol{\varepsilon}}\{\overline{\boldsymbol{\sigma}}\} - W_\square(\boldsymbol{u}\{\overline{\boldsymbol{\sigma}}\})\end{aligned} \tag{38}$$

where the last equality in (38) follows from $(20)_2$ upon choosing the test function $\delta\boldsymbol{t} = \boldsymbol{t}\{\overline{\boldsymbol{\sigma}}\}\in\mathbb{T}_\square$ and from $(27)_3$ upon choosing $\delta\overline{\boldsymbol{\varepsilon}} = \overline{\boldsymbol{\varepsilon}}\{\overline{\boldsymbol{\sigma}}\}$. It can be shown that $\overline{w}_\square^*\{\overline{\boldsymbol{\sigma}}\}$ is a potential for $\overline{\boldsymbol{\varepsilon}}$ in the classical sense, i.e. $\overline{\boldsymbol{\varepsilon}}$ can be obtained as

$$\overline{\boldsymbol{\varepsilon}}\{\overline{\boldsymbol{\sigma}}\} = \frac{\mathrm{d}\overline{w}_\square^*\{\overline{\boldsymbol{\sigma}}\}}{\mathrm{d}\overline{\boldsymbol{\sigma}}} \tag{39}$$

It also follows that $\overline{w}_\square^*\{\overline{\boldsymbol{\sigma}}\}$ is convex in the discrete space $\mathbb{R}_{\mathrm{sym}}^{3\times3}$, and we obtain the Algorithmic Tangent Compliance (ATC)-tensor $\overline{\mathsf{C}}_\square\{\overline{\boldsymbol{\sigma}}\}$ as the positive definite Hessian of $\overline{w}_\square^*\{\overline{\boldsymbol{\sigma}}\}$. Proofs of the various statements above are given in Appendix A.

Remark: In summary, it is possible to relate $\overline{w}_\square\{\overline{\boldsymbol{\varepsilon}}\}$ and $\overline{w}_\square^*\{\overline{\boldsymbol{\sigma}}\}$ via the standard Legendre transformations.

$$\overline{w}_\square^*\{\overline{\boldsymbol{\sigma}}\} = \max_{\widehat{\overline{\boldsymbol{\varepsilon}}}\in\mathbb{R}_{\mathrm{sym}}^{3\times3}} [\overline{\boldsymbol{\sigma}} : \widehat{\overline{\boldsymbol{\varepsilon}}} - \overline{w}_\square\{\widehat{\overline{\boldsymbol{\varepsilon}}}\}] \tag{40}$$

$$\overline{w}_\square\{\overline{\boldsymbol{\varepsilon}}\} = \max_{\widehat{\overline{\boldsymbol{\sigma}}}\in\mathbb{R}_{\mathrm{sym}}^{3\times3}} [\widehat{\overline{\boldsymbol{\sigma}}} : \overline{\boldsymbol{\varepsilon}} - \overline{w}_\square^*\{\widehat{\overline{\boldsymbol{\sigma}}}\}] \tag{41}$$

which turn out to be most useful in the context of constructing energetic bounds.

3.2. Energetic bounds for fixed SVE

We shall consider energetic bounds for $\overline{w}_\square\{\overline{\boldsymbol{\varepsilon}}\}$ and $\overline{w}_\square^*\{\overline{\boldsymbol{\sigma}}\}$ due to the particular restrictions to subspaces of $\mathbb{U}_\square$ and $\mathbb{T}_\square$ that are pertinent to the Dirichlet and Neumann boundary conditions. Henceforth, we use the superscript "D" and "N" for these cases; moreover, we use "T" and "S" to denote the Taylor assumption of vanishing subscale displacement fluctuation and the Sachs assumption of vanishing subscale stress fluctuation inside the SVE.

For the case of macroscale strain control, we recall the inf-sup property in (34). Similarly, for macroscale stress control, we recall the sup-inf-sup property (38). Now, the Neumann problem is characterized by restriction of the traction space such that $\mathbb{U}_\square^N = \mathbb{U}_\square, \mathbb{T}_\square^N \subseteq \mathbb{T}_\square$, the Dirichlet problem is characterized by restriction of the displacement space such that $\mathbb{U}_\square^D \subseteq \mathbb{U}_\square, \mathbb{T}_\square^D = \mathbb{T}_\square$, and the Taylor problem is characterized by $\mathbb{U}_\square^T \subseteq \mathbb{U}_\square^D \subseteq \mathbb{U}_\square, \mathbb{T}_\square^T = \mathbb{T}_\square^D = \mathbb{T}_\square$. We then obtain directly from (34) and (38) the inequalities.

$$\begin{aligned} & \overline{w}_\square^N\{\overline{\boldsymbol{\varepsilon}}\} \;\le\; \overline{w}_\square\{\overline{\boldsymbol{\varepsilon}}\} \;\le\; \overline{w}_\square^D\{\overline{\boldsymbol{\varepsilon}}\} \;\le\; \overline{w}_\square^T\{\overline{\boldsymbol{\varepsilon}}\} \\ \overline{w}_\square^{*T}\{\overline{\boldsymbol{\sigma}}\} \;\le\; & \overline{w}_\square^{*D}\{\overline{\boldsymbol{\sigma}}\} \;\le\; \overline{w}_\square^*\{\overline{\boldsymbol{\sigma}}\} \;\le\; \overline{w}_\square^{*N}\{\overline{\boldsymbol{\sigma}}\} \end{aligned} \tag{42}$$

As an example of the derivation, consider.

---

[10] In the case of a dissipative material this is the incremental strain energy resulting from elimination of internal variables in a timestep.

$$\overline{w}_\square\{\overline{\varepsilon}\} \overset{\text{def}}{=} \inf_{\widehat{\boldsymbol{u}}\in\mathbb{U}_\square}\ \sup_{\widehat{\boldsymbol{t}}\in\mathbb{T}_\square} \Pi_\square(\overline{\varepsilon};\widehat{\boldsymbol{u}},\widehat{\boldsymbol{t}})$$

$$\leq \inf_{\widehat{\boldsymbol{u}}\in\mathbb{U}_\square^D}\ \sup_{\widehat{\boldsymbol{t}}\in\mathbb{T}_\square} \Pi_\square(\overline{\varepsilon};\widehat{\boldsymbol{u}},\widehat{\boldsymbol{t}}) \overset{\text{def}}{=}\overline{w}_\square^D\{\overline{\varepsilon}\} \tag{43}$$

Remark: These bounds hold for any fixed space that may represent the continuous solution or the FE-solution of the SVE-problem for any given (random) realization and finite-sized SVE ($L_\square \leq \infty$). These are the classical bounds; however, it is possible to envision "intermediate" boundary conditions that also give rise to intermediate bounds.

The bounds in (42) are "non-symmetrical" in the sense that the classical lower bound of Sachs (Reuss) is missing for macroscale strain control, while the corresponding upper bound is missing in terms of macroscale stress control. In order to complement the bounds (42), it is necessary to introduce a different variational setting with control of the subscale stress field or, as the alternative, to use a somewhat "ad hoc" strategy. The latter strategy can be outlined as follows:

Consider a given subdivision of $\Omega_\square$ into N subdomains $\Omega_\square = \cup_{i=1}^N \Omega_{)\square(,i}$, and assume that each subdomain $\Omega_{)\square(,i}$ is subjected to the same Neumann condition in terms of the (given) macroscale stress $\overline{\sigma}$. It is then clear that the stress space thus created for the collection of subdomains $\Omega_{)\square(,i}$ is restricted as compared to $\cup_\square^N$ that is valid for the "undivided" $\Omega_\square$. This means that we have the inequality.

$$\overline{w}_\square^{*N}\{\overline{\sigma}\} \leq \frac{1}{N}\sum_{i=1}^N \overline{w}_{)\square(i}^{*N}\{\overline{\sigma}\} \leq \lim_{N\to\infty}\frac{1}{N}\sum_{i=1}^N \overline{w}_{)\square(,i}^{*N}\{\overline{\sigma}\} \overset{\text{def}}{=}\overline{w}_\square^{*S}\{\overline{\sigma}\} \tag{44}$$

The limit value, $\overline{w}_\square^{*S}\{\overline{\sigma}\}$, is denoted the Sachs bound since it effectively amounts to a situation where the stress is constant in $\Omega_\square = \cup_{i=1}^N \Omega_{)\square(,i}$.

Next, we may obtain the strain energy density for given $\overline{\varepsilon}$, denoted $\overline{w}_\square^S\{\overline{\varepsilon}\}$, using a Legendre transformation in (41) and the inequality in (44). We then obtain.

$$\overline{w}_\square^N\{\overline{\varepsilon}\} = \max_{\widehat{\overline{\sigma}}\in\mathbb{R}^{3\times3}_{\text{sym}}} [\widehat{\overline{\sigma}}:\overline{\varepsilon} - \overline{w}_\square^{*N}\{\widehat{\overline{\sigma}}\}]$$

$$\geq \max_{\widehat{\overline{\sigma}}\in\mathbb{R}^{3\times3}_{\text{sym}}} [\widehat{\overline{\sigma}}:\overline{\varepsilon} - \overline{w}_\square^{*S}\{\widehat{\overline{\sigma}}\}] \overset{\text{def}}{=}\overline{w}_\square^S\{\overline{\varepsilon}\} \tag{45}$$

In conclusion, we may complement the bounds in (42) with those in (44) and (45) to, finally, obtain the completed bounds:

$$\begin{aligned}\overline{w}_\square^S\{\overline{\varepsilon}\} &\leq \overline{w}_\square^N\{\overline{\varepsilon}\} \leq \overline{w}_\square\{\overline{\varepsilon}\} \leq \overline{w}_\square^D\{\overline{\varepsilon}\} \leq \overline{w}_\square^T\{\overline{\varepsilon}\}\\ \overline{w}_\square^{*T}\{\overline{\sigma}\} &\leq \overline{w}_\square^{*D}\{\overline{\sigma}\} \leq \overline{w}_\square^*\{\overline{\sigma}\} \leq \overline{w}_\square^{*N}\{\overline{\sigma}\} \leq \overline{w}_\square^{*S}\{\overline{\sigma}\}\end{aligned} \tag{46}$$

3.3. Bounds for the special case of subscale linear elasticity

In the special case that the subscale constituents are characterized by linear elasticity, whereby the effective properties also become linear elastic, we may introduce the effective stiffness tensor $\overline{\mathbf{E}}_\square$ (corresponding to geometrically linear theory) and its inverse $\overline{\mathbf{C}}_\square$ [11] via the explicit expression of the effective strain energy (for given prolongation condition).

---

[11] $\overline{\mathbf{E}}_\square$ has both major and minor symmetry; hence, $\overline{\sigma}$ is symmetrical: Its inverse, $\overline{\mathbf{C}}_\square \overset{\text{def}}{=} [\overline{\mathbf{E}}_\square]^{-1}$, is a mapping between symmetric tensors and has the property $\overline{\mathbf{C}}_\square : \overline{\mathbf{E}}_\square = \overline{\mathbf{I}}^{\text{sym}}$, where $\overline{\mathbf{I}}^{\text{sym}}$ is the standard 4th order tensor with minor symmetry.

$$\overline{w}_\square(\overline{\varepsilon}) = \frac{1}{2}\overline{\varepsilon}:\overline{\mathbf{E}}_\square:\overline{\varepsilon} \quad\Rightarrow\quad \overline{\sigma} = \overline{\mathbf{E}}_\square:\overline{\varepsilon} \tag{47}$$

The strain energies in (46)$_1$ then become.

$$\overline{w}_\square^S(\overline{\varepsilon}) = \frac{1}{2}\overline{\varepsilon}:\overline{\mathbf{E}}_\square^S:\overline{\varepsilon}, \quad \overline{\mathbf{E}}_\square^S \overset{\text{def}}{=} (\langle\mathbf{E}^{-1}\rangle_\square)^{-1}$$

$$\overline{w}_\square^N(\overline{\varepsilon}) = \frac{1}{2}\overline{\varepsilon}:\overline{\mathbf{E}}_\square^N:\overline{\varepsilon}, \quad \overline{w}_\square(\overline{\varepsilon}) = \frac{1}{2}\overline{\varepsilon}:\overline{\mathbf{E}}_\square:\overline{\varepsilon}, \quad \overline{w}_\square^D(\overline{\varepsilon}) = \frac{1}{2}\overline{\varepsilon}:\overline{\mathbf{E}}_\square^D:\overline{\varepsilon},$$

$$\overline{w}_\square^T(\overline{\varepsilon}) = \frac{1}{2}\overline{\varepsilon}:\overline{\mathbf{E}}_\square^T:\overline{\varepsilon}, \quad \overline{\mathbf{E}}_\square^T \overset{\text{def}}{=} \langle\mathbf{E}\rangle_\square \tag{48}$$

whereas the stress energies in (46)$_2$ become

$$\overline{w}_\square^{*T}(\overline{\sigma}) = \frac{1}{2}\overline{\sigma}:\overline{\mathbf{C}}_\square^T:\overline{\sigma}, \quad \overline{\mathbf{C}}_\square^T \overset{\text{def}}{=} (\langle\mathbf{E}\rangle_\square)^{-1}$$

$$\overline{w}_\square^{*D}(\overline{\sigma}) = \frac{1}{2}\overline{\sigma}:\overline{\mathbf{C}}_\square^D:\overline{\sigma}, \quad \overline{w}_\square^*(\overline{\sigma}) = \frac{1}{2}\overline{\sigma}:\overline{\mathbf{C}}_\square:\overline{\sigma}, \quad \overline{w}_\square^{*N}(\overline{\sigma}) = \frac{1}{2}\overline{\sigma}:\overline{\mathbf{C}}_\square^N:\overline{\sigma},$$

$$\overline{w}_\square^{*S}(\overline{\sigma}) = \frac{1}{2}\overline{\sigma}:\overline{\mathbf{C}}_\square^S:\overline{\sigma}, \quad \overline{\mathbf{C}}_\square^S \overset{\text{def}}{=} \langle\mathbf{E}^{-1}\rangle_\square \tag{49}$$

4. Virtual material testing and statistical bounds

4.1. Theoretical bounds on effective energy measures based on finite-sized random SVE:s

The "effective" response is obtained only for infinitely large SVE:s, i.e. for $L_\square \to \infty$. In such a case the boundary conditions do not matter, and we define the true effective response as:

$$\overline{w}\{\overline{\varepsilon}\} = \lim_{L_\square\to\infty}\overline{w}_\square^N\{\overline{\varepsilon}\} = \lim_{L_\square\to\infty}\overline{w}_\square\{\overline{\varepsilon}\} = \lim_{L_\square\to\infty}\overline{w}_\square^D\{\overline{\varepsilon}\} \tag{50}$$

and

$$\overline{w}^*\{\overline{\sigma}\} = \lim_{L_\square\to\infty}\overline{w}_\square^{*D}\{\overline{\sigma}\} = \lim_{L_\square\to\infty}\overline{w}_\square^*\{\overline{\sigma}\} = \lim_{L_\square\to\infty}\overline{w}_\square^{*N}\{\overline{\sigma}\} \tag{51}$$
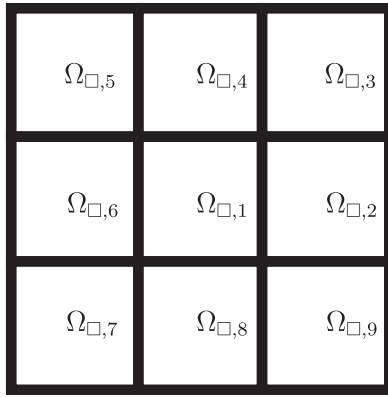
However, it is obviously not feasible to compute results for infinitely large SVE:s; therefore, it is more useful to aim for tight (but still guaranteed) upper and lower bounds on $\overline{w}\{\overline{\varepsilon}\}$ and $\overline{w}^*\{\overline{\sigma}\}$.

In what follows, we adopt a strategy based on arguments on "domain decomposition" and "ergodicity", cf. Zohdi and Wriggers (2005), Hazanov and Huet (1995) and Ostoja-Starzewski (2008). This strategy reminds about the one described for a single realization with "restrictions" in the previous Section; however, with a major difference: Rather than considering smaller subdomains, we now aim at carrying out the computation on a given $\Omega_\square$ with different realizations of the microstructure. We thus consider the "super-SVE" occupying the domain $\Omega_{(\square)}$ of size $L_{(\square)} > L_\square$ with a given (single) realization of the microstructure. The domain $\Omega_{(\square)}$ (e.g. a cube) is now subdivided into N equally sized subdomains $\Omega_{\square,i}, i = 1,2,\ldots,N$ of size $L_\square$ each, i.e. $\Omega_{(\square)} = \cup_{i=1}^N \Omega_{\square,i}$ and $L_{(\square)} = N^{1/d}L_\square$, where d is the space dimension (1,2, or 3), as shown schematically in Fig. 2. Each subdomain $\Omega_{\square,i}(\omega_1), i = 1,2,\ldots,N$ then represents the single realization ω_1 of the stochastic process $\tilde{\omega}$.

The following fundamental inequality can be shown (see Appendix A):

$$\overline{w}\{\overline{\varepsilon}\} = \lim_{L_{(\square)}\to\infty}\overline{w}_{(\square)}^D\{\overline{\varepsilon},\omega_1\} \leq \lim_{N\to\infty}\frac{1}{N}\sum_{j=1}^N \overline{w}_{\square,j}^D\{\overline{\varepsilon},\omega_1\} \tag{52}$$

To proceed, we need an argument on ergodicity. More specifically, it is assumed that the sequence $\Omega_{\square,j}(\omega_1)$ is statistically

Fig. 2. Illustration in 2D of $\Omega_{(\square)}$ consisting of subdomains corresponding to the realizations $\Omega_{\square,i}$ of the statistically homogeneous substructure. The example shows $\Omega_{(\square)} = \cup_{i=1}^{9}\Omega_{\square,i}$.

equivalent to $\Omega_{\square}(\omega_j)$, i.e. the sum in (52) can be replaced by a sum on realizations for the single domain $\Omega_{\square} \stackrel{\text{def}}{=} \Omega_{\square}(\omega_1)$. Hence, the expression in (52) is replaced by[12]

$$\overline{w}\{\overline{\varepsilon}\} \leq \lim_{N \to \infty} \frac{1}{N} \sum_{i=1}^{N} \overline{w}_{\square}^{\mathrm{D}}\{\overline{\varepsilon}, \omega_i\} = E[\overline{w}_{\square}^{\mathrm{D}}\{\overline{\varepsilon}, \tilde{\omega}\}] \stackrel{\text{def}}{=} \overline{w}_{\square}^{\mathrm{D-V}(\infty)}\{\overline{\varepsilon}\}$$
(53)

whereby we note that $\overline{w}_{\square}^{\mathrm{D}}\{\overline{\varepsilon}, \tilde{\omega}\} : \tilde{\omega} \to \mathbb{R}$ is now considered as a stochastic process for given $\overline{\varepsilon}$ and given domain $\Omega_{\square}$.

In a similar fashion as in (52), we may also obtain the following inequality (see Appendix A):

$$\overline{w}^*\{\overline{\sigma}\} = \lim_{L_{(\square)} \to \infty} \overline{w}_{(\square)}^{*\mathrm{N}}\{\overline{\sigma}, \omega_1\} \leq \lim_{N \to \infty} \frac{1}{N} \sum_{j=1}^{N} \overline{w}_{\square,j}^{*\mathrm{N}}\{\overline{\sigma}, \omega_1\}$$
(54)

Hence, by the ergodicity argument, we obtain the "Reuss-type" bound.

$$\overline{w}^*\{\overline{\sigma}\} \leq \lim_{N \to \infty} \frac{1}{N} \sum_{i=1}^{N} \overline{w}_{\square}^{*\mathrm{N}}\{\overline{\sigma}, \omega_i\} = E[\overline{w}_{\square}^{*\mathrm{N}}\{\overline{\sigma}, \tilde{\omega}\}] \stackrel{\text{def}}{=} \overline{w}_{\square}^{*\mathrm{N-R}(\infty)}\{\overline{\sigma}\}$$
(55)

In order to obtain the desired lower bound on $\overline{w}\{\overline{\varepsilon}\}$, we use the Legendre transformation and (55) to obtain.

$$\overline{w}\{\overline{\varepsilon}\} = \max_{\widehat{\overline{\sigma}} \in \mathbb{R}_{\mathrm{sym}}^{3\times3}} [\widehat{\overline{\sigma}} : \overline{\varepsilon} - \overline{w}^*\{\widehat{\overline{\sigma}}\}]$$
$$\geq \max_{\widehat{\overline{\sigma}} \in \mathbb{R}_{\mathrm{sym}}^{3\times3}} [\widehat{\overline{\sigma}} : \overline{\varepsilon} - E[\overline{w}_{\square}^{*\mathrm{N}}\{\widehat{\overline{\sigma}}, \tilde{\omega}\}]] \stackrel{\text{def}}{=} \overline{w}_{\square}^{\mathrm{N-R}(\infty)}\{\overline{\varepsilon}\}$$
(56)

Hence, upon combining (53) and (56), we obtain the theoretical bounds on the effective strain energy density.

$$\overline{w}_{\square}^{\mathrm{N-R}(\infty)}\{\overline{\varepsilon}\} \leq \overline{w}\{\overline{\varepsilon}\} \leq \overline{w}_{\square}^{\mathrm{D-V}(\infty)}\{\overline{\varepsilon}\}$$
(57)

Remark: In order to obtain the "Voigt-type" bound, it is necessary to carry out the Legendre transformation with the purpose to find the stress, denoted $\widetilde{\overline{\sigma}}$, such that $\widetilde{\overline{\sigma}} = \arg[\overline{\varepsilon} - \partial(E[\overline{w}_{\square}^*\{\widehat{\overline{\sigma}}, \tilde{\omega}\}])/\partial\widehat{\overline{\sigma}} = \mathbf{0}]$ for given value of $\overline{\varepsilon}$. In practice, the solution requires some sort of iteration, e.g. Newton iterations.

---

[12] Summation of stiffness properties for a given SVE-size $L_{\square}$ is coined "Voigt-sampling", denoted by superscript "V", whereas summation of flexibility properties is coined "Reuss-sampling", denoted by superscript "R".

It is only in the special case of linear elasticity that no iterations are needed.

Likewise, a lower bound on $\overline{w}^*\{\overline{\sigma}\}$ can be obtained via the Legendre transformation and (53) to obtain.

$$\overline{w}^*\{\overline{\sigma}\} = \max_{\widehat{\overline{\varepsilon}} \in \mathbb{R}_{\mathrm{sym}}^{3\times3}} [\overline{\sigma} : \widehat{\overline{\varepsilon}} - \overline{w}\{\widehat{\overline{\varepsilon}}\}]$$
$$\geq \max_{\widehat{\overline{\varepsilon}} \in \mathbb{R}_{\mathrm{sym}}^{3\times3}} [\overline{\sigma} : \widehat{\overline{\varepsilon}} - E[\overline{w}_{\square}^{\mathrm{D}}\{\widehat{\overline{\varepsilon}}, \tilde{\omega}\}]] \stackrel{\text{def}}{=} \overline{w}_{\square}^{*\mathrm{D-V}(\infty)}\{\overline{\sigma}\}$$
(58)

Hence, upon combining (55) and (58), we obtain the theoretical bounds on the effective stress energy density.

$$\overline{w}_{\square}^{*\mathrm{D-V}(\infty)}\{\overline{\sigma}\} \leq \overline{w}^*\{\overline{\sigma}\} \leq \overline{w}_{\square}^{*\mathrm{N-R}(\infty)}\{\overline{\sigma}\}$$
(59)

4.2. Bounds on effective energy measures for the special case of subscale linear elasticity

In the special case of subscale linear elasticity we obtain for a single realization ω_i

$$\overline{w}_{\square}^{\mathrm{D}}\{\overline{\varepsilon}, \omega_i\} = \frac{1}{2}\overline{\varepsilon} : \overline{\mathbf{E}}_{\square}^{\mathrm{D}}(\omega_i) : \overline{\varepsilon}$$
(60)

$$\overline{w}_{\square}^{*\mathrm{N}}\{\overline{\sigma}, \omega_i\} = \frac{1}{2}\overline{\sigma} : (\overline{\mathbf{E}}_{\square}^{\mathrm{N}}(\omega_i))^{-1} : \overline{\sigma}$$
(61)

whereby the expected value becomes

$$E[\overline{w}_{\square}^{\mathrm{D}}\{\overline{\varepsilon}, \tilde{\omega}\}] = \frac{1}{2}\overline{\varepsilon} : E[\overline{\mathbf{E}}_{\square}^{\mathrm{D}}(\tilde{\omega})] : \overline{\varepsilon}$$
(62)

$$E[\overline{w}_{\square}^{*\mathrm{N}}\{\overline{\sigma}, \tilde{\omega}\}] = \frac{1}{2}\overline{\sigma} : E[(\overline{\mathbf{E}}_{\square}^{\mathrm{N}}(\tilde{\omega}))^{-1}] : \overline{\sigma}$$
(63)

and

$$\overline{w}_{\square}^{\mathrm{D-V}(\infty)}(\overline{\varepsilon}) = \frac{1}{2}\overline{\varepsilon} : \overline{\mathbf{E}}_{\square}^{\mathrm{D-V}(\infty)} : \overline{\varepsilon} \text{ with } \overline{\mathbf{E}}_{\square}^{\mathrm{D-V}(\infty)} \stackrel{\text{def}}{=} E[\overline{\mathbf{E}}_{\square}^{\mathrm{D}}(\tilde{\omega})]$$
$$\overline{w}_{\square}^{\mathrm{N-R}(\infty)}(\overline{\varepsilon}) = \frac{1}{2}\overline{\varepsilon} : \overline{\mathbf{E}}_{\square}^{\mathrm{N-R}(\infty)} : \overline{\varepsilon} \text{ with } \overline{\mathbf{E}}_{\square}^{\mathrm{N-R}(\infty)} \stackrel{\text{def}}{=} (E[(\overline{\mathbf{E}}_{\square}^{\mathrm{N}}(\tilde{\omega}))^{-1}])^{-1}$$
(64)

$$\overline{w}_{\square}^{*\mathrm{N-R}(\infty)}(\overline{\sigma}) = \frac{1}{2}\overline{\sigma} : \overline{\mathbf{C}}_{\square}^{\mathrm{N-R}(\infty)} : \overline{\sigma} \text{ with } \overline{\mathbf{C}}_{\square}^{\mathrm{N-R}(\infty)} \stackrel{\text{def}}{=} (\overline{\mathbf{E}}_{\square}^{\mathrm{N-R}(\infty)})^{-1}$$
$$\overline{w}_{\square}^{*\mathrm{D-V}(\infty)}(\overline{\sigma}) = \frac{1}{2}\overline{\sigma} : \overline{\mathbf{C}}_{\square}^{\mathrm{D-V}(\infty)} : \overline{\sigma} \text{ with } \overline{\mathbf{C}}_{\square}^{\mathrm{D-V}(\infty)} \stackrel{\text{def}}{=} (\overline{\mathbf{E}}_{\square}^{\mathrm{D-V}(\infty)})^{-1}$$
(65)

4.3. Statistical bounds on effective energy measures

4.3.1. General situation − computable bounds

The results derived so far in this paper are to a large extent classical in the sense that they can be found in the literature, although not in the variational framework and not in the complete setup shown here. However, these developments will be crucial as the point of departure for the truly novel discussion below:

In practice, it is possible to compute expected values, denoted $E[\bullet]$, to lie in a certain *given confidence interval* only. For given probability $\overline{P}$ the confidence interval in terms of $c[\bullet]$ is defined such that $P(|E[\bullet] - \mu[\bullet]| \leq c) = \overline{P}$, where $\mu[\bullet]$ is the mean value.

Obviously, $c[\bullet]$ decreases with increasing number of realizations, N. The required probability affects both the mean value and the number of required realizations for a given confidence interval, i.e. for given bounds. The higher the value of $\overline{P}$ is, the more accurate is $\mu[\bullet]$ at the expense of larger N.

Hence, rather than aiming for the bounds in (57) and (59), which are non-computable, we shall aim for *computable upper and lower bounds* on $\overline{w}\{\overline{\varepsilon}\}$ and $\overline{w}^*\{\overline{\sigma}\}$.

4.3.2. Statistical upper and lower bounds on strain energy − an assessment of different strategies

The computable bounds on $\overline{w}\{\overline{\varepsilon}\}$ are denoted $\overline{w}_\square^{UB}\{\overline{\varepsilon}\}$ and $\overline{w}_\square^{LB}\{\overline{\varepsilon}\}$, respectively. This means that (57) is replaced by.

$$\overline{w}_\square^{LB}\{\overline{\varepsilon}\} \leq \overline{w}\{\overline{\varepsilon}\} \leq \overline{w}_\square^{UB}\{\overline{\varepsilon}\} \tag{66}$$

Firstly, in order to compute the upper bound, $\overline{w}_\square^{UB}\{\overline{\varepsilon}\}$, we use the inequality.

$$\overline{w}\{\overline{\varepsilon}\} \leq E[\overline{w}_\square^{D}\{\overline{\varepsilon}, \tilde{\omega}\}]$$
$$\leq \mu[\overline{w}_\square^{D}\{\overline{\varepsilon}, \omega_i\}_{i=1}^{N}] + c[\overline{w}_\square^{D}\{\overline{\varepsilon}, \omega_i\}_{i=1}^{N}, \overline{P}] \stackrel{\text{def}}{=} \overline{w}_\square^{UB}\{\overline{\varepsilon}\} \tag{67}$$

Secondly, in order to compute the lower bound (or, rather, any lower bound), $\overline{w}_\square^{LB}\{\overline{\varepsilon}\}$, we first use that (for any given $\overline{\sigma}$)

$$E[\overline{w}_\square^{*N}\{\overline{\sigma}, \tilde{\omega}\}] \leq \mu[\overline{w}_\square^{*N}\{\overline{\sigma}, \omega_i\}_{i=1}^{N}] + c[\overline{w}_\square^{*N}\{\overline{\sigma}, \omega_i\}_{i=1}^{N}, \overline{P}] \tag{68}$$

whereby it is noted that, for the same value of c in (67) and (68), the required value of N may be different. A lower bound can then be obtained, upon combining the last row in (56) with (68), as follows:

$$\overline{w}\{\overline{\varepsilon}\} \geq \widetilde{\overline{\sigma}} : \overline{\varepsilon} - \mu[\overline{w}_\square^{*N}\{\widetilde{\overline{\sigma}}, \omega_i\}_{i=1}^{N}] - c[\overline{w}_\square^{*N}\{\widetilde{\overline{\sigma}}, \omega_i\}_{i=1}^{N}, \overline{P}] \stackrel{\text{def}}{=} \overline{w}_\square^{LB}\{\overline{\varepsilon}\} \tag{69}$$

for *any given choice* of $\widetilde{\overline{\sigma}} \in \mathbb{R}_{\text{sym}}^{3\times3}$.

Obviously, the actual choice of $\widetilde{\overline{\sigma}} \in \mathbb{R}_{\text{sym}}^{3\times3}$ may produce a more or less sharp bound while giving rize to a more or less complex computation. Subsequently, we list a few viable options starting with the "sharpest" one:

1. Optimal choice.

$$\widetilde{\overline{\sigma}}\{\overline{\varepsilon}\} = \arg \max_{\widehat{\overline{\sigma}} \in \mathbb{R}_{\text{sym}}^{3\times3}} [\widehat{\overline{\sigma}} : \overline{\varepsilon} - \mu[\overline{w}_\square^{*N}\{\widehat{\overline{\sigma}}, \omega_i\}_{i=1}^{N}] - c[\overline{w}_\square^{*N}\{\widehat{\overline{\sigma}}, \omega_i\}_{i=1}^{N}, \overline{P}]] \tag{70}$$

For given value of $\overline{\varepsilon}$, this is a nonlinear optimization problem in $\widetilde{\overline{\sigma}}$; hence, its solution will be quite cumbersome and non-tractable in practice, even in the case of linear elasticity. However, the resulting value of $\widetilde{\overline{\sigma}}$ is optimal in the sense that it produces the sharpest possible bound when inserted in (69).

2. Neumann−Reuss stress − quasi-optimal choice.

$$\widetilde{\overline{\sigma}}(\overline{\varepsilon}) = \arg \max_{\widehat{\overline{\sigma}} \in \mathbb{R}_{\text{sym}}^{3\times3}} [\widehat{\overline{\sigma}} : \overline{\varepsilon} - \mu[\overline{w}_\square^{*N}\{\widehat{\overline{\sigma}}, \omega_i\}_{i=1}^{N}]] \tag{71}$$

The resulting solution is denoted $\widetilde{\overline{\sigma}}\{\overline{\varepsilon}\} = \overline{\sigma}_\square^{N-R(N)}\{\overline{\varepsilon}\}$. This choice is obviously identical to the optimal one when $c \to 0$.

3. Neumann−Voigt stress (approximation of Neumann−Reuss stress).

$$\widetilde{\overline{\sigma}}(\overline{\varepsilon}) = \mu[\overline{\sigma}_\square^{N}\{\overline{\varepsilon}, \omega_i\}_{i=1}^{N}] \stackrel{\text{def}}{=} \overline{\sigma}_\square^{N-V(N)}\{\overline{\varepsilon}\} \quad \text{with } \overline{\sigma}_\square^{N}\{\overline{\varepsilon}\} \stackrel{\text{def}}{=} \frac{\partial \overline{w}_\square^{N}\{\overline{\varepsilon}\}}{\partial \overline{\varepsilon}} \tag{72}$$

That this is an approximation of the quasi-optimal choice is shown as follows:

$$\max_{\widehat{\overline{\sigma}} \in \mathbb{R}_{\text{sym}}^{3\times3}} [\widehat{\overline{\sigma}} : \overline{\varepsilon} - \mu[\overline{w}_\square^{*N}\{\widehat{\overline{\sigma}}, \omega_i\}_{i=1}^{N}]]$$
$$= \max_{\widehat{\overline{\sigma}} \in \mathbb{R}_{\text{sym}}^{3\times3}} [\widehat{\overline{\sigma}} : \overline{\varepsilon} - \mu[\max_{\widehat{\overline{\varepsilon}} \in \mathbb{R}_{\text{sym}}^{3\times3}} [\widehat{\overline{\sigma}} : \widehat{\overline{\varepsilon}} - \overline{w}_\square^{N}\{\widehat{\overline{\varepsilon}}, \omega_i\}_{i=1}^{N}]]]$$
$$\approx \max_{\widehat{\overline{\sigma}} \in \mathbb{R}_{\text{sym}}^{3\times3}} [\widehat{\overline{\sigma}} : \overline{\varepsilon} - \max_{\widehat{\overline{\varepsilon}} \in \mathbb{R}_{\text{sym}}^{3\times3}} [\widehat{\overline{\sigma}} : \widehat{\overline{\varepsilon}} - \mu[\overline{w}_\square^{N}\{\widehat{\overline{\varepsilon}}, \omega_i\}_{i=1}^{N}]]]$$
$$= \max_{\widehat{\overline{\sigma}} \in \mathbb{R}_{\text{sym}}^{3\times3}} \min_{\widehat{\overline{\varepsilon}} \in \mathbb{R}_{\text{sym}}^{3\times3}} [\widehat{\overline{\sigma}} : \overline{\varepsilon} - \widehat{\overline{\sigma}} : \widehat{\overline{\varepsilon}} + \mu[\overline{w}_\square^{N}\{\widehat{\overline{\varepsilon}}, \omega_i\}_{i=1}^{N}]]$$

Carrying out the variation w.r.t. $\widehat{\overline{\varepsilon}}$ infers that $\widehat{\overline{\sigma}} = \overline{\sigma}_\square^{N-V(N)}\{\widehat{\overline{\varepsilon}}\}$, whereas a variation w.r.t. $\widehat{\overline{\sigma}}$ infers that $\widehat{\overline{\varepsilon}} = \overline{\varepsilon}$. We thus obtain the proposed result. It is noted that the approximation introduced in the derivation above stems from the assumption that the maximization in $\widehat{\overline{\varepsilon}}$ has the same solution for each realization.

4. Dirichlet−Voigt stress.

$$\widetilde{\overline{\sigma}}(\overline{\varepsilon}) = \mu[\overline{\sigma}_\square^{D}\{\overline{\varepsilon}, \omega_i\}_{i=1}^{N}] \stackrel{\text{def}}{=} \overline{\sigma}_\square^{D-V(N)}\{\overline{\varepsilon}\} \quad \text{with } \overline{\sigma}_\square^{D}\{\overline{\varepsilon}\} \stackrel{\text{def}}{=} \frac{\partial \overline{w}_\square^{D}\{\overline{\varepsilon}\}}{\partial \overline{\varepsilon}} \tag{73}$$

5. Voigt stress.

$$\widetilde{\overline{\sigma}}(\overline{\varepsilon}) = \langle \sigma(\overline{\varepsilon}) \rangle_\square \stackrel{\text{def}}{=} \overline{\sigma}_\square^{V}(\overline{\varepsilon}) \tag{74}$$

This is the stress obtained from the Taylor assumption, which does not require the solution of any SVE-problem.

6. Stress calculation for any single SVE-realization subjected to any choice of boundary conditions.

It is possible to choose the macroscale stress $\widetilde{\overline{\sigma}}(\overline{\varepsilon}) = \overline{\sigma}$ from any single SVE-realization. The chosen boundary conditions may be arbitrary: Dirichlet, Neumann, strongly periodic or weakly periodic.

Remark: Apart from the "optimal choice" it is not possible to establish a strict hierarchy of the methods listed above from purely theoretical estimates; however, numerical assessment will give a hint. One may expect a trade-off between computational cost and accuracy, cf. the numerical evaluation below.

We summarize the formulation of the upper and lower bounds as

$$\overline{w}_\square^{UB}\{\overline{\varepsilon}\} = \overline{w}_\square^{D-V(N)}\{\overline{\varepsilon}\} + c[\overline{w}_\square^{D}\{\overline{\varepsilon}, \omega_i\}_{i=1}^{N}, \overline{P}] \tag{75}$$

$$\overline{w}_\square^{LB}\{\overline{\varepsilon}\} = \overline{w}_\square^{N-R(N)}\{\overline{\varepsilon}\} - c[\overline{w}_\square^{*N}\{\widetilde{\overline{\sigma}}(\overline{\varepsilon}), \omega_i\}_{i=1}^{N}, \overline{P}] \tag{76}$$

where we introduced the auxiliary notation

$$\overline{w}_\square^{D-V(N)}\{\overline{\varepsilon}\} = \mu[\overline{w}_\square^D\{\overline{\varepsilon}, \omega_i\}_{i=1}^N] \tag{77}$$

$$\overline{w}_\square^{N-R(N)}\{\overline{\varepsilon}\} = \widetilde{\overline{\sigma}}(\overline{\varepsilon}) : \overline{\varepsilon} - \mu[\overline{w}_\square^{*N}\{\widetilde{\overline{\sigma}}(\overline{\varepsilon}), \omega_i\}_{i=1}^N] \tag{78}$$

corresponding to the Voigt and Reuss sampling strategies.

4.3.3. Statistical upper and lower bounds on stress energy

The computable bounds on $\overline{w}^*\{\overline{\sigma}\}$ are denoted $\overline{w}_\square^{*UB}\{\overline{\sigma}\}$ and $\overline{w}_\square^{*LB}\{\overline{\sigma}\}$, respectively. This means that (59) is replaced by.

$$\overline{w}_\square^{*LB}\{\overline{\sigma}\} \leq \overline{w}^*\{\overline{\sigma}\} \leq \overline{w}_\square^{*UB}\{\overline{\sigma}\} \tag{79}$$

In order to compute the upper bound, $\overline{w}_\square^{*UB}\{\overline{\sigma}\}$, we use the inequality.

$$\begin{aligned}
\overline{w}^*\{\overline{\sigma}\} &\leq E[\overline{w}_\square^{*N}\{\overline{\sigma}, \tilde{\omega}\}] \\
&\leq \mu[\overline{w}_\square^{*N}\{\overline{\sigma}, \omega_i\}_{i=1}^N] + c[\overline{w}_\square^{*N}\{\overline{\sigma}, \omega_i\}_{i=1}^N, \overline{P}] \stackrel{def}{=} \overline{w}_\square^{*UB}\{\overline{\sigma}\}
\end{aligned} \tag{80}$$

In order to compute the lower bound (or, rather, any lower bound), $\overline{w}_\square^{*LB}\{\overline{\sigma}\}$, we first use that (for any given $\overline{\varepsilon}$)

$$E[\overline{w}_\square^D\{\overline{\varepsilon}, \tilde{\omega}\}] \leq \mu[\overline{w}_\square^D\{\overline{\varepsilon}, \omega_i\}_{i=1}^N] + c[\overline{w}_\square^D\{\overline{\varepsilon}, \omega_i\}_{i=1}^N, \overline{P}] \tag{81}$$

whereby it is noted that, for the same value of c in (80) and (81), the required value of N may be different. A lower bound can then be obtained, upon combining the last row in (58) with (81), as follows:

$$\overline{w}^*\{\overline{\sigma}\} \geq \overline{\sigma} : \widetilde{\overline{\varepsilon}} - \mu[\overline{w}_\square^D\{\widetilde{\overline{\varepsilon}}, \omega_i\}_{i=1}^N] - c[\overline{w}_\square^D\{\widetilde{\overline{\varepsilon}}, \omega_i\}_{i=1}^N, \overline{P}] \stackrel{def}{=} \overline{w}_\square^{*LB}\{\overline{\sigma}\} \tag{82}$$

for any given choice of $\widetilde{\overline{\varepsilon}} \in \mathbb{R}_{sym}^{3 \times 3}$.

In a similar fashion as for the strain energy, the actual choice of $\widetilde{\overline{\varepsilon}} \in \mathbb{R}_{sym}^{3 \times 3}$ may produce a more or less sharp bound while giving rise to a more or less complex computation.

4.4. Statistical bounds on strain and stress energies for the special case of subscale linear elasticity

In the special case that the subscale constituents are characterized by linear elasticity, we first recall the expressions in (60), (61), and we obtain the mean values.

$$\mu[\overline{w}_\square^D\{\overline{\varepsilon}, \omega_i\}_{i=1}^N] = \frac{1}{2}\overline{\varepsilon} : \mu[\overline{\mathbf{E}}_\square^D(\omega_i)_{i=1}^N] : \overline{\varepsilon} \tag{83}$$

$$\mu[\overline{w}_\square^{*N}\{\overline{\sigma}, \omega_i\}_{i=1}^N\}] = \frac{1}{2}\overline{\sigma} : \mu\left[((\overline{\mathbf{E}}_\square^N(\omega_i))^{-1})_{i=1}^N\right] : \overline{\sigma} \tag{84}$$

In order to obtain an explicit expression for the lower bound, we adopt the "quasi-optimal" approach, whereby we obtain the explicit solution $\widetilde{\overline{\sigma}}(\overline{\varepsilon}) = \overline{\mathbf{E}}_\square^{N-R(N)} : \overline{\varepsilon}$ upon carrying out the maximization in (71). We remark that this is precisely the Neumann–Reuss approximation; hence, the method denoted "Neumann–Reuss approximation" gives the same result as the quasi-optimal method in the particular case of linear elasticity. From the definitions in (77) and (78) combined with (83) and, (84), we thus obtain for the strain-controlled setting.

$$\overline{w}_\square^{D-V(N)}(\overline{\varepsilon}) = \frac{1}{2}\overline{\varepsilon} : \overline{\mathbf{E}}_\square^{D-V(N)} : \overline{\varepsilon} \quad \text{with} \quad \overline{\mathbf{E}}_\square^{D-V(N)} = \mu[\overline{\mathbf{E}}_\square^D(\omega_i)_{i=1}^N]$$

$$\overline{w}_\square^{N-R(N)}(\overline{\varepsilon}) = \frac{1}{2}\overline{\varepsilon} : \overline{\mathbf{E}}_\square^{N-R(N)} : \overline{\varepsilon} \quad \text{with} \quad \overline{\mathbf{E}}_\square^{N-R(N)} = (\mu[((\overline{\mathbf{E}}_\square^N(\omega_i))^{-1})_{i=1}^N])^{-1} \tag{85}$$

We also obtain

$$c[\overline{w}_\square^D\{\overline{\varepsilon}, \omega_i\}_{i=1}^N, \overline{P}] = c[(\frac{1}{2}\overline{\varepsilon} : \overline{\mathbf{E}}_\square^D(\omega_i) : \overline{\varepsilon})_{i=1}^N, \overline{P}] \tag{86}$$

$$c[\overline{w}_\square^{*N}\{\widetilde{\overline{\sigma}}(\overline{\varepsilon}), \omega_i\}_{i=1}^N, \overline{P}] = c[\overline{\overline{w}}_\square^N\{\overline{\varepsilon}, \omega_i\}_{i=1}^N, \overline{P}] \stackrel{def}{=} c[(\frac{1}{2}\overline{\varepsilon} : \overline{\overline{\mathbf{E}}}_\square^N(\omega_i) : \overline{\varepsilon})_{i=1}^N, \overline{P}] \tag{87}$$

where we introduced the scaled effective free energy and stiffness tensor for an individual realization

$$\begin{aligned}
\overline{\overline{w}}_\square^N\{\overline{\varepsilon}, \omega_i\} &= \frac{1}{2}\overline{\varepsilon} : \overline{\overline{\mathbf{E}}}_\square^N(\omega_i) : \overline{\varepsilon}, \quad \overline{\overline{\mathbf{E}}}_\square^N(\omega_i) \stackrel{def}{=} \overline{\mathbf{E}}_\square^{N-R(N)} : (\overline{\mathbf{E}}_\square^N(\omega_i))^{-1} \\
&: \overline{\mathbf{E}}_\square^{N-R(N)}
\end{aligned} \tag{88}$$

Analogous results can be obtained for the stress-controlled format.

4.5. Statistical bounds on material parameters for assumed macroscale isotropic linear elasticity

A quite restrictive *assumption* is that the effective (macroscopic) properties are characterized by isotropic linear elasticity, i.e.

$$\overline{\mathbf{E}} = 2\overline{G}\mathbf{I}_{dev}^{sym} + \overline{K}\mathbf{I} \otimes \mathbf{I}, \quad \overline{\mathbf{C}} \stackrel{def}{=} \overline{\mathbf{E}}^{-1} = \frac{1}{2\overline{G}}\mathbf{I}_{dev}^{sym} + \frac{1}{9\overline{K}}\mathbf{I} \otimes \mathbf{I} \tag{89}$$

where $\overline{G}$, $\overline{K}$ are the effective elastic shear and bulk modulus, respectively. It must be noted that it is only the effective properties, i.e. for $L_\square = \infty$, that are isotropic (for any choice of boundary conditions on the SVE). In other words, the effective moduli $\overline{\mathbf{E}}_\square$, $\overline{\mathbf{E}}_\square^D$, $\overline{\mathbf{E}}_\square^N$, etc. for finite-size single SVE-realizations do not represent isotropic response. It is possible to obtain bounds directly on $\overline{G}$ and $\overline{K}$ by using the general procedure above and utilizing the expressions for the energy bounds in (77) and (78) in a quite straightforward fashion; however, it is also possible to obtain a (slightly sharper)[13] lower bound by directly using the assumed macroscale isotropy. This alternative will be shown next.

Upon introducing the dimensionless "deformation modes"

$$\overline{\varepsilon}_G \stackrel{def}{=} \frac{\overline{\varepsilon}_{dev}}{|\overline{\varepsilon}_{dev}|}, \quad \overline{\varepsilon}_{dev} \stackrel{def}{=} \overline{\varepsilon} - \frac{1}{3}[\mathbf{I} : \overline{\varepsilon}]\mathbf{I} \tag{90}$$

$$\overline{\varepsilon}_K \stackrel{def}{=} \frac{\overline{\varepsilon}_{vol}}{|\overline{\varepsilon}_{vol}|}, \quad \overline{\varepsilon}_{vol} \stackrel{def}{=} \frac{1}{3}[\mathbf{I} : \overline{\varepsilon}]\mathbf{I} \tag{91}$$

and the dimensionless "stress modes" $\overline{\sigma}_G = 2\overline{\varepsilon}_G$, $\overline{\sigma}_K = \sqrt{2}\overline{\varepsilon}_K$, we first obtain directly from (89)

---

[13] It does not seem possible to show rigorously that the present approach gives a sharper lower bound; however, the numerical results confirm this hypothesis (presumption).

$$\overline{G} = \overline{w}_\square(\overline{\boldsymbol{\varepsilon}}_G), \quad \frac{1}{\overline{G}} = \overline{w}_\square^*(\overline{\boldsymbol{\sigma}}_G) \tag{92}$$

$$\overline{K} = \overline{w}_\square(\overline{\boldsymbol{\varepsilon}}_K), \quad \frac{1}{\overline{K}} = \overline{w}_\square^*(\overline{\boldsymbol{\sigma}}_K) \tag{93}$$

In this case we may replace (66) by.

$$\overline{G}_\square^{LB} \leq \overline{G} \leq \overline{G}_\square^{UB}, \quad \overline{K}_\square^{LB} \leq \overline{K} \leq \overline{K}_\square^{UB} \tag{94}$$

where $\overline{G}_\square^{LB}, \overline{G}_\square^{UB}$ and $\overline{K}_\square^{LB}, \overline{K}_\square^{UB}$ are the computable bounds for a finite-sized SVE. Henceforth we consider bounds for $\overline{G}$ only (since those of $\overline{K}$ are completely similar).

In order to compute the upper bound, $\overline{G}_\square^{UB}$, we use the first identity in (92) to obtain.

$$\overline{G} \leq E[\overline{w}_\square^D\{\overline{\boldsymbol{\varepsilon}}_G, \tilde{\omega}\}]$$
$$\leq \mu[\overline{w}_\square^D\{\overline{\boldsymbol{\varepsilon}}_G, \omega_i\}_{i=1}^N] + c[\overline{w}_\square^D\{\overline{\boldsymbol{\varepsilon}}_G, \omega_i\}_{i=1}^N, \overline{P}] \overset{\text{def}}{=} \overline{G}_\square^{UB} \tag{95}$$

In order to compute the lower bound (or, rather, a particular lower bound), $\overline{G}_\square^{LB}$, we use the second identity in (92) to obtain.

$$\overline{G} \geq \frac{1}{E[\overline{w}_\square^{*N}\{\overline{\boldsymbol{\sigma}}_G, \tilde{\omega}\}]}$$
$$\geq \frac{1}{\mu[\overline{w}_\square^{*N}\{\overline{\boldsymbol{\sigma}}_G, \omega_i\}_{i=1}^N] + c[\overline{w}_\square^{*N}\{\overline{\boldsymbol{\sigma}}_G, \omega_i\}_{i=1}^N, \overline{P}]} \overset{\text{def}}{=} \overline{G}_\square^{LB} \tag{96}$$

The definitions of $\overline{w}_\square^D\{\overline{\boldsymbol{\varepsilon}}, \omega_i\}$ and $\overline{w}_\square^{*N}\{\overline{\boldsymbol{\sigma}}, \omega_i\}$ were given in (60) and (61), respectively.

Finally, the upper and lower bounds on the effective shear modulus are expressed as follows:

$$\overline{G}_\square^{UB} = \mu[\overline{G}_\square^D(\omega_i)_{i=1}^N] + c[\overline{G}_\square^D(\omega_i)_{i=1}^N, \overline{P}] \tag{97}$$

$$\overline{G}_\square^{LB} = \frac{1}{\mu[(\overline{G}_\square^N)^{-1}(\omega_i)_{i=1}^N] + c[(\overline{G}_\square^N)^{-1}(\omega_i)_{i=1}^N, \overline{P}]} \tag{98}$$

where we introduced the "apparent shear moduli"

$$\overline{G}_\square^D \overset{\text{def}}{=} \overline{w}_\square^D(\overline{\boldsymbol{\varepsilon}}_G), \quad \overline{G}_\square^N \overset{\text{def}}{=} \frac{1}{\overline{w}_\square^{*N}(\overline{\boldsymbol{\sigma}}_G)} \tag{99}$$

Quite similar expressions can be obtained for $\overline{K}_\square^{UB}$ and $\overline{K}_\square^{LB}$.

Remark: The upper bound $\overline{G}_\square^{UB}$ is identical to $\overline{w}_\square^{UB}(\overline{\boldsymbol{\varepsilon}}_G)$, as defined in (75), while the lower bound $\overline{G}_\square^{LB}$ differs from $\overline{w}_\square^{LB}(\overline{\boldsymbol{\varepsilon}}_G)$ in general and does not involve the additional computation of any stress $\tilde{\overline{\boldsymbol{\sigma}}}$, as discussed for the general approach.

5. Computational examples

5.1. Subscale modeling − SVE-design

We consider a microstructure composed of round (cylindrical in the presently considered 2D-case) and stiff particles (p) in a compliant matrix material (m). The particle diameter is denoted d_p, which is henceforth taken as the reference length of the substructure; $L_{ref} = d_p$. Moreover, the mean volume fraction of particles is $n_p = 0.40$. In terms of a topologically cubic (square in the presently considered 2D-case) array of particles, this volume fraction corresponds to a mean particle distance that is certainly larger than d_p. For each realization of the microstructure, particles are positioned within the SVE in a random fashion, and typical such

random realizations are shown in Fig. 3 for $L_\square/L_{ref} = 1.25, 2.50$ and 5.00.

As to the subscale displacement FE-mesh, it is aligned with the topology. An alternative would be to represent the microstructural features according to the "multiphase elements" strategy, whereby phase properties are assigned to the individual Gauss integration points, cf. Schmauder et al. (1996) or Quilici and Cailletaud (1999). However, the representation of the matrix/inclusion interface would then be strongly affected by the mesh density.

5.2. Subscale modeling − constitutive properties

5.2.1. Canonical variational format of a dissipative material

The mesoscale material properties of a dissipative material are characterized by two volume-specific potentials: the free energy $\psi(\boldsymbol{\varepsilon}, \underline{k})$ and the (dual) dissipation potential $\phi^*(\underline{\kappa})$. The adopted framework is sufficiently general to contain (visco)plasticity as the prototype model (whose specifics are given in the next Subsection). From $\psi(\boldsymbol{\varepsilon}, \underline{k})$ we identify the equilibrium stress $\boldsymbol{\sigma}$ and the dissipative stress $\underline{\kappa}$, which are given as the state functions ("reversible stresses" in the nomenclature of Nguyen, 2010).

$$\boldsymbol{\sigma}(\boldsymbol{\varepsilon}, \underline{k}) \overset{\text{def}}{=} \frac{\partial \psi(\boldsymbol{\varepsilon}, \underline{k})}{\partial \boldsymbol{\varepsilon}}, \quad \underline{\kappa}(\boldsymbol{\varepsilon}, \underline{k}) \overset{\text{def}}{=} -\frac{\partial \psi(\boldsymbol{\varepsilon}, \underline{k})}{\partial \underline{k}} \tag{100}$$

The evolution rule for the internal variables $\underline{k} \in \mathbb{R}^N$ is expressed as.

$$\underline{\dot{k}} = \frac{\partial \phi^*}{\partial \underline{\kappa}}(\underline{\kappa}) \tag{101}$$

Adopting the standard Backward Euler (BE) rule to integrate (101) in the time interval $(t_{n-1}, t_n = t_{n-1} + \Delta t)$, we may solve for the time-updated fields, $\underline{k}(\boldsymbol{x}), \underline{\kappa}(\boldsymbol{x})^{14}$ for given value of $\boldsymbol{\varepsilon}$, from the time discrete equations:

$$\frac{\partial \psi(\boldsymbol{\varepsilon}, \underline{k})}{\partial \underline{k}} + \underline{\kappa} = \underline{0} \tag{102}$$

$$\underline{k} - \Delta t \frac{\partial \phi^*}{\partial \underline{\kappa}}(\underline{\kappa}) = {}^{n-1}\underline{k} \tag{103}$$

These equations represent the stationarity conditions of the problem.

$$(\underline{k}, \underline{\kappa}) = \arg\left\{ \min_{\widehat{\underline{k}} \in \mathbb{R}^N} \max_{\widehat{\underline{\kappa}} \in \mathbb{R}^N} \pi(\boldsymbol{\varepsilon}; \widehat{\underline{k}}, \widehat{\underline{\kappa}}) \right\} \tag{104}$$

where the volume-specific incremental potential π is given as

$$\pi(\boldsymbol{\varepsilon}; \underline{k}, \underline{\kappa}) = \psi(\boldsymbol{\varepsilon}, \underline{k}) - {}^{n-1}\psi + \underline{\kappa}*[\underline{k} - {}^{n-1}\underline{k}] - \Delta t \Phi^*(\underline{\kappa}) \tag{105}$$

In other words, the conditions (102) and (103) are identical to.

$$\pi_k'(\boldsymbol{\varepsilon}; \underline{k}, \underline{\kappa}; \delta\underline{k}) = [\frac{\partial \psi(\boldsymbol{\varepsilon}, \underline{k})}{\partial \underline{k}} + \underline{\kappa}]^T \delta\underline{k} = 0 \quad \forall \delta\underline{k} \in \mathbb{R}^N, \tag{106}$$

$$\pi_k'(\boldsymbol{\varepsilon}; \underline{k}, \underline{\kappa}; \delta\underline{\kappa}) = [\underline{k} - {}^{n-1}\underline{k} - \Delta t \frac{\partial \phi^*}{\partial \underline{\kappa}}(\underline{\kappa})]^T \delta\underline{\kappa} = 0 \quad \forall \delta\underline{\kappa} \in \mathbb{R}^N \tag{107}$$

This problem can be solved for $\underline{k}\{\boldsymbol{\varepsilon}\}$ and $\underline{\kappa}\{\boldsymbol{\varepsilon}\} \overset{\text{def}}{=} \underline{\kappa}(\boldsymbol{\varepsilon}, \underline{k}\{\boldsymbol{\varepsilon}\})$ for any given $\boldsymbol{\varepsilon}$. In such a case we obtain the volume-specific incremental pseudo-elastic strain energy as the saddle-point value of π, for any given $\boldsymbol{\varepsilon}$, as.

---

[14] $\boldsymbol{u}(\boldsymbol{x}) \overset{\text{def}}{=} {}^n\boldsymbol{u}(\boldsymbol{x})$ etc., i.e. superindex ^{n} is dropped for brevity.

$$\frac{L_\square}{L_{\text{ref}}} = 1.25 \qquad \frac{L_\square}{L_{\text{ref}}} = 2.50 \qquad \frac{L_\square}{L_{\text{ref}}} = 5.00$$
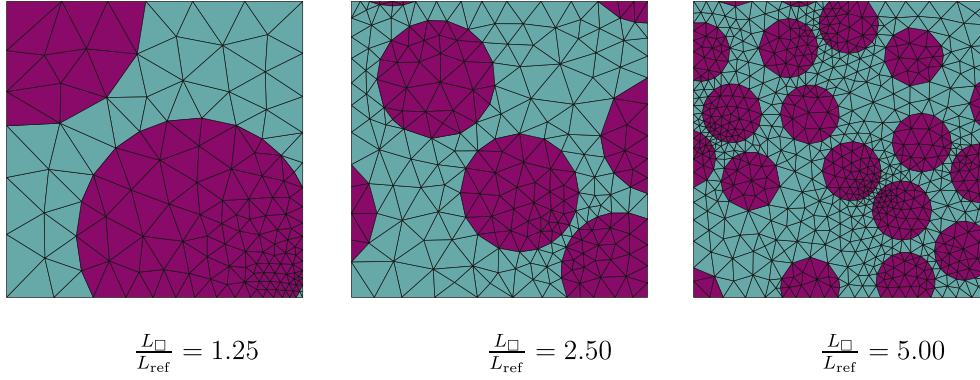
Fig. 3. Single realization of random microstructure for different SVE-sizes.

$$w\{\boldsymbol{\varepsilon}\} \stackrel{\text{def}}{=} \pi(\boldsymbol{\varepsilon}, \underline{k}\{\boldsymbol{\varepsilon}\}, \underline{\kappa}\{\boldsymbol{\varepsilon}\})$$
$$= \psi(\boldsymbol{\varepsilon}, \underline{k}\{\boldsymbol{\varepsilon}\}) - {}^{n-1}\psi + \underline{\kappa}\{\boldsymbol{\varepsilon}\}^{\text{T}}[\underline{k}\{\boldsymbol{\varepsilon}\} - {}^{n-1}\underline{k}] - \Delta t\phi^*(\underline{\kappa}\{\boldsymbol{\varepsilon}\})$$

(108)

that serves as the potential for $\boldsymbol{\sigma}\{\boldsymbol{\varepsilon}\}$ in the given time interval, i.e.

$$dw\{\boldsymbol{\varepsilon}\} = \left.\frac{\partial\psi(\boldsymbol{\varepsilon}, \underline{k}\{\boldsymbol{\varepsilon}\})}{\partial\boldsymbol{\varepsilon}}\right|_{\underline{k}} : d\boldsymbol{\varepsilon} = \boldsymbol{\sigma}\{\boldsymbol{\varepsilon}\} : d\boldsymbol{\varepsilon}$$

(109)

The corresponding algorithmic stiffness tensor (ATS-tensor) becomes:

$$d\boldsymbol{\sigma}\{\boldsymbol{\varepsilon}\} = \mathbf{E}_{\text{T}}\{\boldsymbol{\varepsilon}\} : d\boldsymbol{\varepsilon}$$

(110)

with the definition

$$\mathbf{E}_{\text{T}} = \frac{d^2 w\{\boldsymbol{\varepsilon}\}}{d\boldsymbol{\varepsilon} \otimes d\boldsymbol{\varepsilon}} = \left.\frac{\partial^2\psi(\boldsymbol{\varepsilon}, \underline{k}\{\boldsymbol{\varepsilon}\})}{\partial\boldsymbol{\varepsilon} \otimes \partial\boldsymbol{\varepsilon}}\right|_{\underline{k}} + \left.\frac{\partial^2\psi(\boldsymbol{\varepsilon}, \underline{k}\{\boldsymbol{\varepsilon}\})}{\partial\boldsymbol{\varepsilon} \otimes \partial\underline{k}^{\text{T}}}\right|_{\boldsymbol{\varepsilon}} \underline{k}'\{\boldsymbol{\varepsilon}\}$$

(111)

Here we introduced the sensitivity in the sense that the (implicit) relation $\underline{k}\{\boldsymbol{\varepsilon}\}$ is linearized to give $\underline{k}'\{\boldsymbol{\varepsilon}; d\boldsymbol{\varepsilon}\} = \underline{\boldsymbol{k}}'\{\boldsymbol{\varepsilon}\} : d\boldsymbol{\varepsilon}$.

In order to obtain an operational version of the canonical format that comprises (visco)plasticity, we define the elastic domain $\mathbb{E}$ as.

$$\mathbb{E} = \{\underline{\kappa}| \ \phi_{\text{P}}^*(\underline{\kappa}) \le 0\}$$

(112)

where $\phi_{\text{P}}^*(\underline{\kappa})$ is a convex "threshold function" (or quasistatic yield function in terms of the nomenclature of viscoplasticity). Typically, we express $\phi^*(\underline{\kappa}) = (1/t_*)\eta(\phi_{\text{P}}^*(\underline{\kappa}))$, where t_* is a relaxation (time) parameter, and the scalar "overstress" function $\eta(x)$ is required to possess the properties $\eta'(x) \ge 0$ for $x \ge 0$ and $\eta'(x) = 0$ for $x \le 0$. Hence, the evolution rule for $\underline{k}$ in (101) is expressed as

$$\underline{\dot{k}} = \lambda(\underline{\kappa})\frac{\partial\phi_{\text{P}}^*}{\partial\underline{\kappa}}(\underline{\kappa}) \quad \text{with} \quad \lambda(\underline{\kappa}) \stackrel{\text{def}}{=} \frac{1}{t_*}\eta'(\phi_{\text{P}}^*(\underline{\kappa}))$$

(113)

The time-updated fields $\underline{k}(\boldsymbol{x}), \underline{\kappa}(\boldsymbol{x}), \gamma(\boldsymbol{x})$ are computed from the time-discrete equations, for given $\boldsymbol{\varepsilon}$,

$$\underline{k} - \gamma\frac{\partial\phi_{\text{P}}^*}{\partial\underline{\kappa}}(\underline{\kappa}(\boldsymbol{\varepsilon}, \underline{k})) = {}^{n-1}\underline{k}$$

(114)

$$\frac{t_*}{\Delta t}\gamma - \eta'(\phi_{\text{P}}^*(\underline{\kappa}(\boldsymbol{\varepsilon}, \underline{k}))) = 0$$

(115)

5.2.2. Prototype model of viscoplasticity with linear isotropic hardening

We consider a standard viscoplasticity model of the Bingham type with isotropic hardening to represent the subscale material response. The model is defined by two internal variables $k = \{\boldsymbol{\varepsilon}^{\text{p}}, k\}$, where $\boldsymbol{\varepsilon}^{\text{p}}$ is the plastic (part of) strain and k is the variable that represents isotropic hardening. The elastic strain is then given as $\boldsymbol{\varepsilon}^{\text{e}}(\boldsymbol{\varepsilon}, \boldsymbol{\varepsilon}^{\text{p}}) \stackrel{\text{def}}{=} \boldsymbol{\varepsilon} - \boldsymbol{\varepsilon}^{\text{p}}$. The free energy is proposed as

$$\psi(\boldsymbol{\varepsilon}^{\text{e}}(\boldsymbol{\varepsilon}, \boldsymbol{\varepsilon}^{\text{p}}), k) = \frac{1}{2}\left[3G[e(\boldsymbol{\varepsilon}^{\text{e}})]^2 + K[v(\boldsymbol{\varepsilon}^{\text{e}})]^2\right] + \frac{1}{2}Hk^2$$

(116)

In (116) we used the effective elastic strain $e(\boldsymbol{\varepsilon}^{\text{e}})$ and the volumetric elastic strain $v(\boldsymbol{\varepsilon}^{\text{e}})$ via the definitions $e(\boldsymbol{\varepsilon}) \stackrel{\text{def}}{=} \sqrt{2/3}|\boldsymbol{\varepsilon}_{\text{dev}}|$ and $v(\boldsymbol{\varepsilon}) \stackrel{\text{def}}{=} \boldsymbol{\varepsilon} : \boldsymbol{I}$, and the decomposition $\boldsymbol{\varepsilon} = \boldsymbol{\varepsilon}_{\text{dev}} + (1/3)v(\boldsymbol{\varepsilon})\boldsymbol{I}$. The material parameters are the (state-independent but generally spatially inhomogeneous) elastic moduli G, K, and the hardening modulus H.

From (116) we obtain the constitutive state equations as follows:

$$\boldsymbol{\sigma} = \boldsymbol{\sigma}_{\text{dev}} + \sigma_{\text{m}}\boldsymbol{I} \quad \text{with} \quad \boldsymbol{\sigma}_{\text{dev}} = 2G\boldsymbol{\varepsilon}_{\text{dev}}^{\text{e}}, \sigma_{\text{m}} = Kv(\boldsymbol{\varepsilon}^{\text{e}})$$

(117)

$$\boldsymbol{\sigma}^{\text{p}} \stackrel{\text{def}}{=} -\frac{\partial\psi^*}{\partial\boldsymbol{\varepsilon}^{\text{p}}}[=\boldsymbol{\sigma}], \quad \kappa \stackrel{\text{def}}{=} -\frac{\partial\psi^*}{\partial k} = -Hk$$

(118)

The loading function expressing isotropic hardening is given as

$$\phi_{\text{P}}^*(\boldsymbol{\sigma}, \kappa) = s(\boldsymbol{\sigma}) - Y - \kappa$$
$$= s(\boldsymbol{\sigma}(\boldsymbol{\varepsilon}, \boldsymbol{\varepsilon}^{\text{p}})) - Y + Hk = 3Ge(\boldsymbol{\varepsilon}^{\text{e}}) - Y + Hk$$

(119)

where $s(\boldsymbol{\sigma}) \stackrel{\text{def}}{=} \sqrt{3/2}|\boldsymbol{\sigma}_{\text{dev}}|$ is the effective stress, whereas Y is the quasistatic yield stress (material parameter). We also choose the simple "overstress" model

$$\phi^* = \frac{1}{t_*}\eta(\phi_{\text{P}}^*) \quad \text{with} \quad \eta(\phi_{\text{P}}^*) = \frac{1}{2Y}\langle\phi_{\text{P}}^*\rangle^2$$

(120)

and we obtain

$$\frac{\partial\phi^*}{\partial\boldsymbol{\sigma}} = \lambda\frac{3\boldsymbol{\sigma}_{\text{dev}}}{2s(\boldsymbol{\sigma})} = \lambda\frac{\boldsymbol{\varepsilon}_{\text{dev}}^{\text{e}}}{e(\boldsymbol{\varepsilon}^{\text{e}})}$$

(121)

$$\frac{\partial\phi^*}{\partial\kappa} = -\lambda$$

(122)

where the "plastic multiplier" state function is given as

$$\lambda = \frac{1}{t_* Y} \langle \phi_P^*(e(\varepsilon^e), k) \rangle \tag{123}$$

From (114) it is possible to express the time-updated values of the two internal variables ε^p and k in terms of ε^e and $\gamma \overset{\text{def}}{=} \lambda \Delta t$:

$$\varepsilon^p = {}^{n-1}\varepsilon^p + \gamma \frac{\varepsilon_{dev}^e}{e(\varepsilon^e)} = {}^{n-1}\varepsilon^p + \gamma \frac{\varepsilon_{dev}^{e,tr}}{e(\varepsilon^{e,tr})} \text{ with } \varepsilon^{e,tr} \overset{\text{def}}{=} {}^{n-1}\varepsilon^e + \Delta\varepsilon \tag{124}$$

$$k = {}^{n-1}k - \gamma \tag{125}$$

The scalar γ is the solution of the constitutive equation (115)

$$\frac{t_*}{\Delta t} Y \gamma - \langle \phi_P^*(\varepsilon^{e,tr}, \gamma) \rangle = 0 \tag{126}$$

where

$$\phi_P^*(\varepsilon^{e,tr}, \gamma) = (\phi_P^*)^{tr}(\varepsilon^{e,tr}) - h^p \gamma \quad \text{with} \quad h^p \overset{\text{def}}{=} 3G + H \tag{127}$$

and where the "trial value" of the loading function ϕ_P^* corresponding to pure elastic incremental response is given as

$$(\phi_P^*)^{tr}(\varepsilon^{e,tr}) \overset{\text{def}}{=} 3Ge(\varepsilon^{e,tr}) - Y + H\,{}^{n-1}k. \tag{128}$$

Inelastic loading at any spatial point $x \in \Omega$ is characterized by $\phi_P^* > 0$, whereby γ can be solved from (126) as.

$$\gamma = \frac{(\phi_P^*)^{tr}}{h^{vp}} \quad \text{with} \quad h^{vp} \overset{\text{def}}{=} h^p + \frac{t_*}{\Delta t} Y \tag{129}$$

Finally, the volume-specific incremental potential in (105) takes the explicit form.

$$\pi(\varepsilon; \varepsilon^p, k, \sigma, \kappa) = \psi(\varepsilon, \varepsilon^p, k) - {}^{n-1}\psi + \sigma$$
$$: [\varepsilon^p - {}^{n-1}\varepsilon^p] + \kappa[k - {}^{n-1}k] - \Delta t \phi^*(\sigma, \kappa) \tag{130}$$

where we have the parametrization $\sigma(\varepsilon, \gamma)$, $\varepsilon^p(\varepsilon, \gamma)$, $k(\gamma)$, $\kappa(\gamma)$.

5.2.2.1. Special case: Hencky plasticity. Hencky-type deformation plasticity is retrieved as the (incremental) response in a single (the first) timestep for the rate-independent version of the Bingham model, defined by $t_* = 0$. This situation is characterized by the simplifications $\psi n - 1 = 0$, ${}^{n-1}\varepsilon^p = \mathbf{0}$, $kn - 1 = 0$. With the notation $\varepsilon_e \overset{\text{def}}{=} e(\varepsilon^{sym}) = \sqrt{2/3} \left| \varepsilon_{dev}^{sym} \right|$ and $\varepsilon_v \overset{\text{def}}{=} v(\varepsilon) = \varepsilon : \mathbf{I}$, the volume-specific pseudo-elastic strain energy then becomes.

$$w(\varepsilon) = w_{dev}(\varepsilon_e) + w_{vol}(\varepsilon_v) \tag{131}$$

whereby the energy is split into the "deviatoric" and "volumetric" parts

$$w_{dev}(\varepsilon_e) = \begin{cases} \dfrac{3G}{2}[\varepsilon_e]^2 & \text{if } \varepsilon_e \leq \dfrac{Y}{3G} \\ \dfrac{3G}{2}[\varepsilon_e]^2 - \dfrac{h^p}{2}\left[\dfrac{3G\varepsilon_e - Y}{h^p}\right]^2 & \text{if } \varepsilon_e > \dfrac{Y}{3G} \end{cases} \tag{132}$$

$$w_{vol}(\varepsilon_v) = \frac{1}{2}K\varepsilon_v^2 \tag{133}$$

We then obtain

$$\sigma(\varepsilon) = \frac{dw(\varepsilon)}{d\varepsilon} = 2G^*(\varepsilon_e)\varepsilon_{dev}^{sym} + K\varepsilon_v \mathbf{I} \tag{134}$$

where the (current) secant shear modulus G^* is given as

$$G^*(\varepsilon_e) = \begin{cases} G & \text{if } \varepsilon_e \leq \dfrac{Y}{3G} \\ G\left[1 - \dfrac{\gamma(\varepsilon_e)}{\varepsilon_e}\right] & \text{if } \varepsilon_e > \dfrac{Y}{3G} \end{cases} \tag{135}$$

5.3. Computational results − purely elastic response

The first series of computational results are obtained for purely elastic response, and we evaluate bounds on the (volume-specific) strain energy. The elastic moduli, G, K, are expressed in terms of the modulus of elasticity, E, and Poisson's ratio, v, as $G = E/2[1 + v]$, $K = E/3[1 - 2v]$. The chosen parameter values for the subsequent computational comparison are shown in Table 1. They represent an "academic" material in the sense that the ratio of E for particles and matrix material was chosen unrealistically high in order to "provoke" discriminating results with respect to the micro-heterogeneity.

Firstly, we consider uniaxial strain defined by $\bar{\varepsilon}_A = \bar{\varepsilon}\mathbf{e}_1 \otimes \mathbf{e}_1$. The energy values are scaled with the reference value $\overline{w}_{\square,ref} = E_{ref}\bar{\varepsilon}^2$. Fig. 4 shows how the (scaled) mean value of the strain energy $\overline{w}_\square$ for this particular deformation mode converges with increasing SVE-size. The corresponding mean values of $\overline{w}_\square$ for the application of Reuss and Voigt sampling on the weakly periodic boundary conditions are also shown in this figure. Confidence intervals are also shown, corresponding to 1% of the mean value with 95% probability, i.e. we choose N such that $c = 0.01\mu[\bullet]$ and $\overline{P} = 0.95$.

To obtain an even more complete comparison, we note that the mean energy value pertinent to the Taylor and Sachs assumptions are (typically) $\overline{w}_\square^T / \overline{w}_{\square,ref} \approx 4.68$ and $\overline{w}_\square^S / \overline{w}_{\square,ref} \approx 1.67$, respectively, and these values are quite insensitive to the SVE-size. It is noted that the value of $\overline{w}_\square^T$ is way off from the "converged range", obtained for large $L_\square$, whereas the value of $\overline{w}_\square^S$ is much closer. However, this result is probably heavily dependent on the fact that a case of hard particles in a soft matrix is studied. It is also noted that there seems to be an "optimal balance" of the displacement and traction discretization that ensures very fast convergence with increasing SVE-size.

The number of realizations, N, required to achieve the targeted confidence interval (1%) with given probability (95%) in Fig. 4, depends strongly on the SVE-size. Fig. 5 shows how N decreases with increasing SVE-size for different boundary conditions.
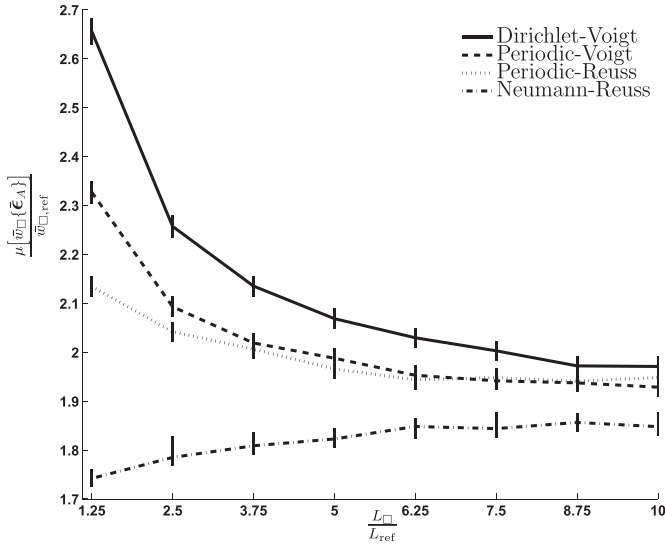
In order to check the effect of randomized microstructure, the development of the (scaled) standard deviation of $\overline{w}_\square$ with SVE-size is shown in Fig. 6. For large SVE-sizes, quite few realizations are needed and the standard deviation is also very small. This is in agreement with the fact that larger SVE-sizes are statistically representative for the effective properties.

The upper and lower bounds for $\overline{w}_\square\{\bar{\varepsilon}_A\}$ depend on the prescribed probability used for the computation of confidence

Table 1
Actual parameter values. E_{ref} is a suitable reference modulus, representing the matrix material.

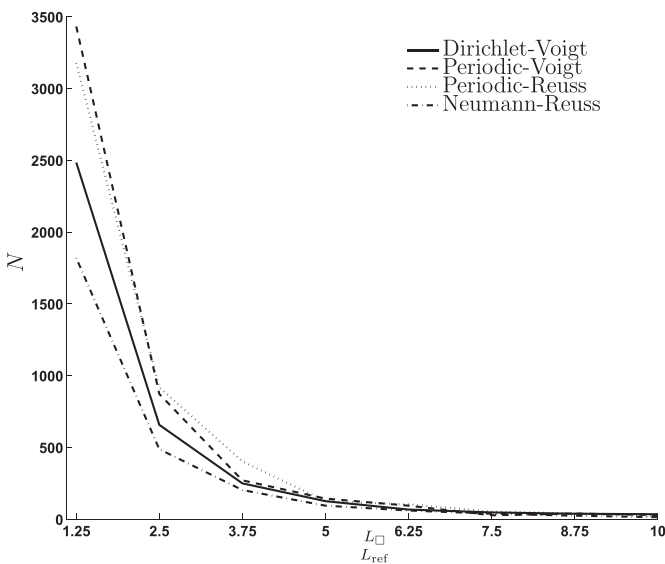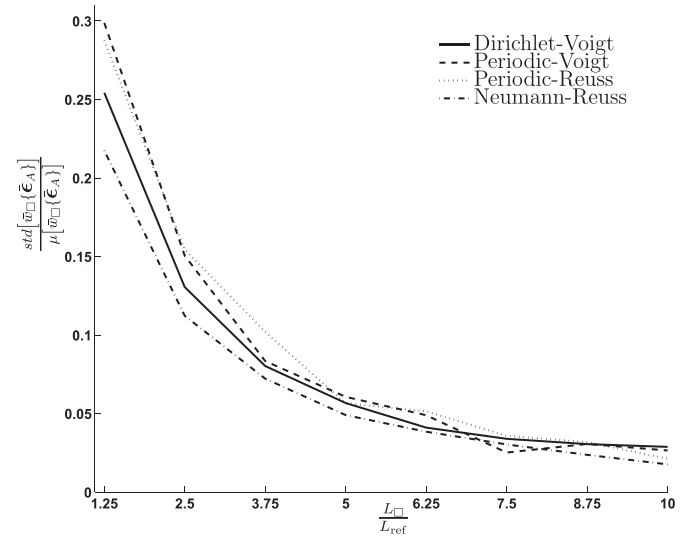|	E/E_{ref}	v
Particles	15	0.30
Matrix	1	0.40

Fig. 4. Convergence of mean value of strain energy $\overline{w}_\square\{\overline{\varepsilon}_A\}$ with SVE-size. Results are shown for a given fixed displacement mesh, but for different boundary conditions and sampling strategies (e.g. Dirichlet b.c. and Voigt sampling). Confidence intervals of 1% are indicated by vertical lines for each SVE-size.

Fig. 6. Convergence of (scaled) standard deviation of strain energy $\overline{w}_\square\{\overline{\varepsilon}_A\}$ with SVE-size. Results are shown for a fixed displacement mesh, but for different boundary conditions and sampling strategies.

intervals. This fact is clearly visible in Fig. 7, wherein the convergence of the (scaled) upper and lower bounds of the strain energy $\overline{w}_\square\{\overline{\varepsilon}_A\}$ are shown for different prescribed confidence levels, $\overline{P}$. In this Figure, the same sequence of realizations, representing given mean value and standard deviation, is utilized for the computation of the upper and lower bounds for the different confidence levels.

In Fig. 8, the convergence of the mean value of the strain energy with SVE-size is shown for Dirichlet and Neumann boundary conditions with Reuss and Voigt sampling strategies. It is noted that the results obtained from different boundary conditions with Reuss and Voigt sampling, respectively, tend to the classical Reuss and Voigt bounds for SVE:s smaller than a certain size. In other words, regardless of the boundary condition used for the SVE-problem, adopting Reuss and Voigt sampling strategies for asymptotically
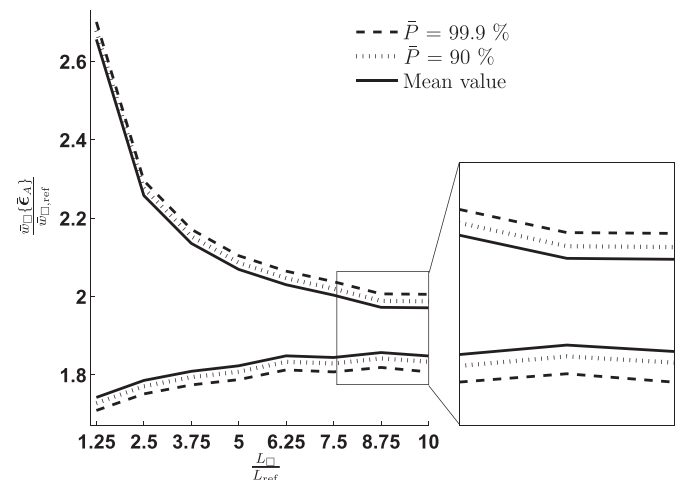
zero-size SVE:s results in mean values corresponding to, respectively, homogeneous stress and strain fields.

Results are also presented for pure shear deformation, defined by $\overline{\varepsilon}_B = (\overline{\gamma}/2)[\boldsymbol{e}_1 \otimes \boldsymbol{e}_2 + \boldsymbol{e}_2 \otimes \boldsymbol{e}_1]$. For the value $\overline{\gamma} = \sqrt{2}$, then $|\overline{\varepsilon}_B| = 1$, and $\overline{w}_\square\{\overline{\varepsilon}_B\} = \overline{G}_\square$, cf. (92). In this case we choose to scale with E_{ref}. Figs. 9 and 10 are then completely analogous to Figs. 4 and 8.

Finally, different approaches for computation of the lower bounds are compared in Fig. 11. It is noted that the strategy that is based on the presumption of isotropic macroscopic stiffness gives rise to a sharper lower bound on $\overline{G}_\square$. For the assumed macroscopic isotropy, no optimization problem need be solved and, therefore, the results are different from the general case.
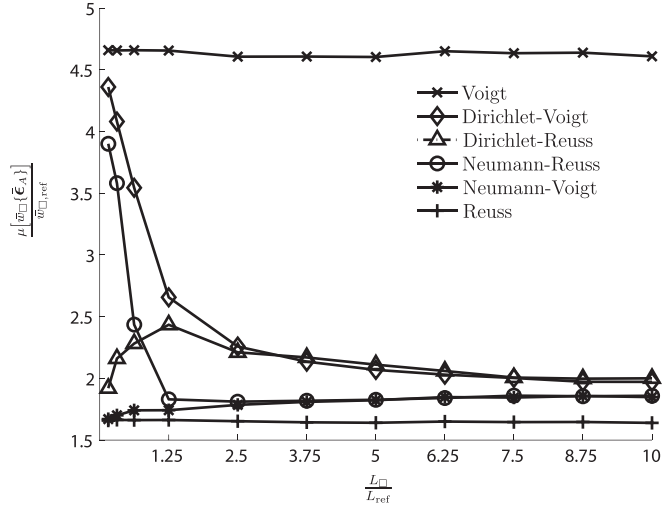
5.4. Computational results — elastic-plastic response

The second series of results are obtained for nonlinear response. The chosen parameter values for the subsequent computational comparison are shown in Table 2, and they represent typical data for a composite with steel particles embedded in an aluminum matrix ($E_{\text{ref}} = 70$ GPa). In this case, we choose the confidence interval as 0.5% of the mean value with 95% probability.

Fig. 5. Development of the number of realizations N, required to estimate $\overline{w}_\square\{\overline{\varepsilon}_A\}$ within the given confidence interval, with SVE-size. Results are given for fixed displacement mesh, but for different boundary conditions and sampling strategies.

Fig. 7. Convergence of the (scaled) upper and lower bounds for $\overline{w}_\square\{\overline{\varepsilon}_A\}$ with SVE-size. Results are given for different prescribed levels of confidence (value of $\overline{P}$).
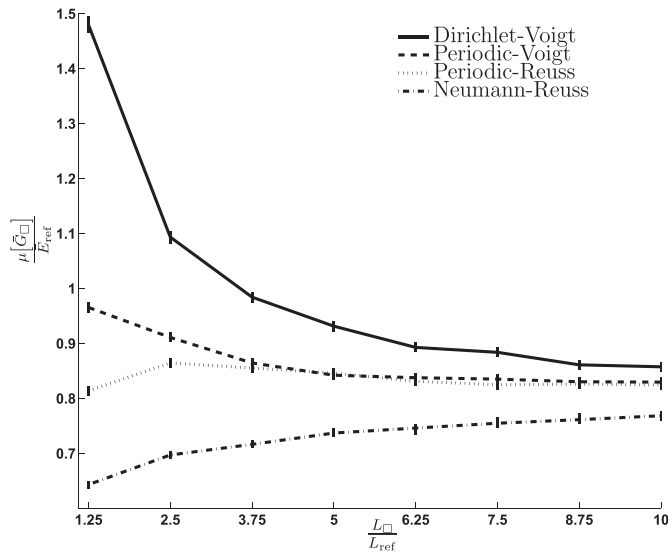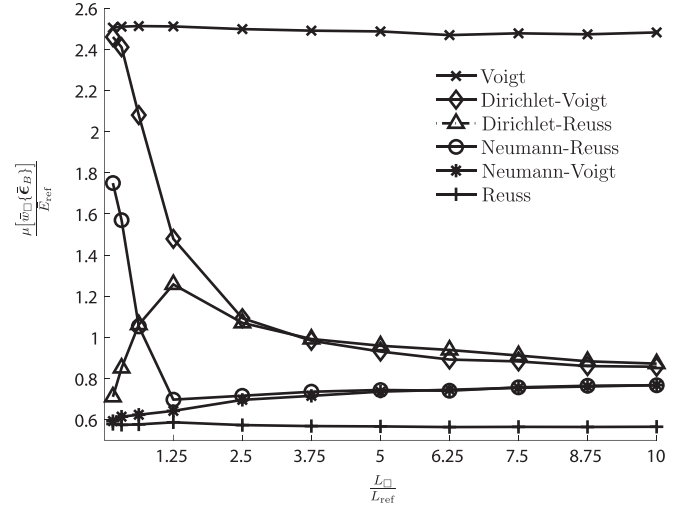
Fig. 8. Convergence of the (scaled) strain energy $\overline{w}_\square\{\overline{\varepsilon}_A\}$ with SVE-size. Results are given for Dirichlet and Neumann boundary conditions with Reuss and Voigt sampling strategies.

Fig. 10. Convergence of the (scaled) strain energy $\overline{w}_\square\{\overline{\varepsilon}_B\}$ with SVE-size. Results are given for Dirichlet and Neumann boundary conditions with Reuss and Voigt sampling strategies.

Firstly, we assess the effectiveness of (some of) the different methods for computing the lower bound $\overline{w}_\square^{LB}$ in terms of different ways of computing the stress $\widetilde{\overline{\sigma}}$, as discussed in Subsection 4.3.2. Fig. 12 shows three different options that all lead to guaranteed lower bounds but are approximations of the optimal (sharpest) lower bound. For completeness the classical Reuss lower bound is also shown. As expected, the "suboptimal" method based on Neumann—Voigt sampling, defined in Eq. (72), gives the sharpest bound.
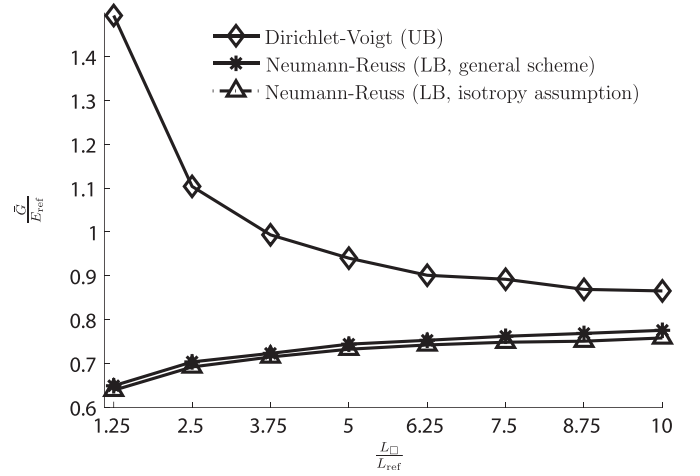
Secondly, we show the typical convergence of upper and lower bounds, $\overline{w}_\square^{UB}$ and $\overline{w}_\square^{LB}$, with increasing SVE-size in Fig. 13. In view of the result in Fig. 12, the "sub-optimal" method based on Neumann—Voigt sampling for computing the stress $\widetilde{\overline{\sigma}}$ is chosen to obtain the lower bound. The mean values based on Dirichlet—Voigt and Neumann—Reuss sampling are shown as well. For

Fig. 11. Convergence of upper and lower bounds of strain energy $\overline{w}_\square\{\overline{\varepsilon}_B\}$ with SVE-size. Results are shown for a given fixed displacement mesh and for different strategies to compute the lower bound (while assuming macroscale isotropy and adopting the general scheme, respectively).

completeness the classical Voigt upper bound, denoted $\overline{w}_\square^V$, and the corresponding Reuss lower bound, obtained via Legendre transformation and denoted $\overline{w}_\square^R$, are also shown. It must be noted that these latter (classical) bounds are the theoretical ones that are computed based on the theoretical value of volume fractions for each realization and each SVE-size. The investigation is carried out for the fixed uniaxial macroscopic strain $\overline{\varepsilon} = 0.005\boldsymbol{e}_1 \otimes \boldsymbol{e}_1$.

Thirdly, in Fig. 14 we assess the effectiveness of a deceivingly straightforward approximation of the lower bound, denoted $\overline{w}_\square^{LB,appr}\{\overline{\varepsilon}\}$ and defined as the "Neumann—Voigt"-type of measure.
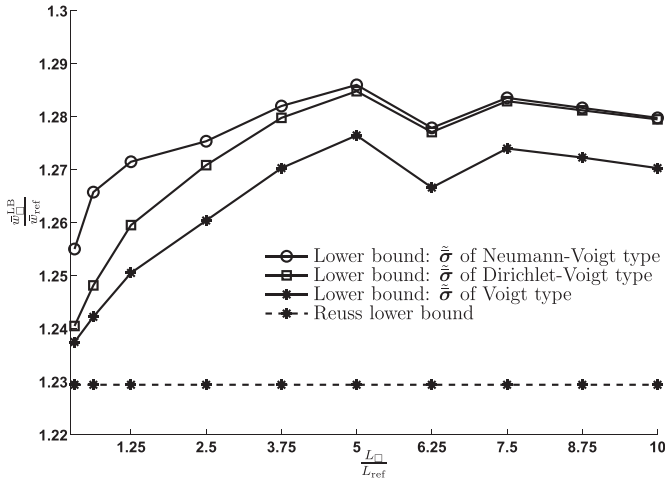

Fig. 9. Convergence of mean value of strain energy $\overline{w}_\square\{\overline{\varepsilon}_B\}$ with SVE-size. Results are shown for a given fixed displacement mesh, but for different boundary conditions and sampling strategies. Confidence intervals of 1% are indicated by vertical lines for each SVE-size.

$$\overline{w}_\square^{LB,appr}\{\overline{\boldsymbol{\varepsilon}}\} \overset{\text{def}}{=} \mu[\overline{w}_\square^N\{\overline{\boldsymbol{\varepsilon}}, \omega_i\}_{i=1}^N] \qquad (136)$$

It turns out that $\overline{w}_\square^{LB,appr}\{\overline{\boldsymbol{\varepsilon}}\}$ is larger than the optimal lower bound (and thus larger than any other guaranteed lower bounds as those discussed in Subsection 4.3.2). This is shown as follows:
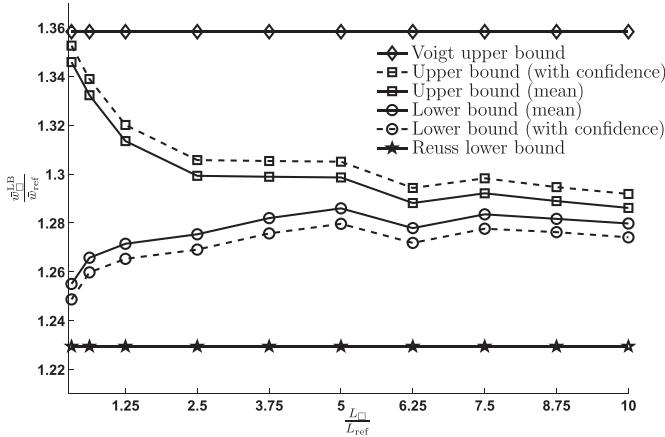
Table 2
Actual parameter values. E_{ref} is a suitable reference modulus, representing the matrix material.

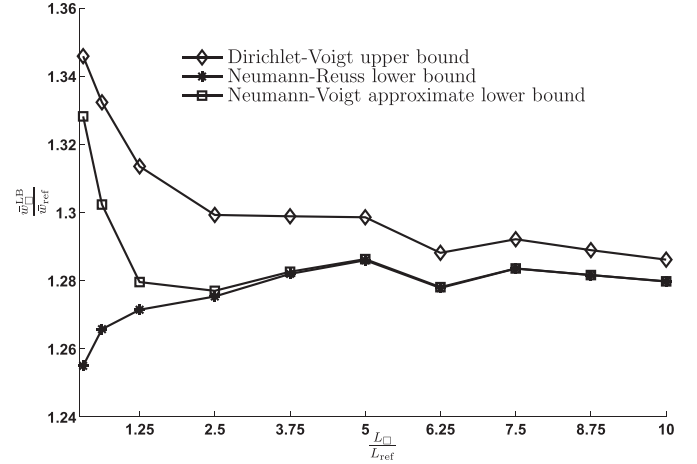|	E/E_{ref}	ν	H/E_{ref}	Y/E_{ref}
Particles	3	0.30	0.385	0.005
Matrix	1	0.40	0.119	0.003

Fig. 12. Convergence of the lower bound on the strain energy, $\overline{w}_{\square}^{\text{LB}}$, with SVE-size. Results are shown for a given fixed mesh, and for different choices of $\tilde{\tilde{\sigma}}$ to obtain an approximate lower bound. $\tilde{\overline{\varepsilon}} = \overline{\varepsilon}e_1 \otimes e_1$ with $\overline{\varepsilon} = 0.005$. All curves show mean values, i.e. Neumann–Reuss sampling. The (theoretical) Reuss lower bound is shown for comparison.

Fig. 13. Convergence of upper and lower bounds on the strain energy, $\overline{w}_{\square}^{\text{UB}}$ and $\overline{w}_{\square}^{\text{LB}}$, with SVE-size. Results are shown for a given fixed mesh, and for the Neumann–Voigt method of computing $\tilde{\tilde{\sigma}}$ in order to obtain an approximate lower bound. $\tilde{\overline{\varepsilon}} = \overline{\varepsilon}e_1 \otimes e_1$ with $\overline{\varepsilon} = 0.005$.

$$\overline{w}_{\square}^{\text{LB,appr}}\{\overline{\varepsilon}\} = \frac{1}{N}\sum_{i=1}^{N}\overline{w}^{\text{N}}\{\overline{\varepsilon},\omega_i\} = \frac{1}{N}\sum_{i=1}^{N}[\max_{\hat{\overline{\sigma}}_i \in \mathbb{R}_{\text{sym}}^{3\times3}}[\widehat{\overline{\sigma}}_i:\overline{\varepsilon} - \overline{w}_{\square}^{*\text{N}}\{\widehat{\overline{\sigma}}_i,\omega_i\}]]$$

$$\geq \max_{\hat{\overline{\sigma}} \in \mathbb{R}_{\text{sym}}^{3\times3}}[\frac{1}{N}\sum_{i=1}^{N}[\widehat{\overline{\sigma}}:\overline{\varepsilon} - \overline{w}_{\square}^{*\text{N}}\{\widehat{\overline{\sigma}},\omega_i\}]]] = \max_{\hat{\overline{\sigma}} \in \mathbb{R}_{\text{sym}}^{3\times3}}[\widehat{\overline{\sigma}}:\overline{\varepsilon} - \mu[\overline{w}_{\square}^{*\text{N}}\{\widehat{\overline{\sigma}},\omega_i\}_{i=1}^{N}]]$$

$$\geq \overline{w}_{\square}^{\text{LB}}\{\overline{\varepsilon}\}$$

(137)

The last identity follows from a comparison with the definition of $\overline{w}_{\square}^{\text{LB}}\{\overline{\varepsilon}\}$ in (69) while choosing the optimal value of $\tilde{\tilde{\sigma}}\{\overline{\varepsilon}\}$.
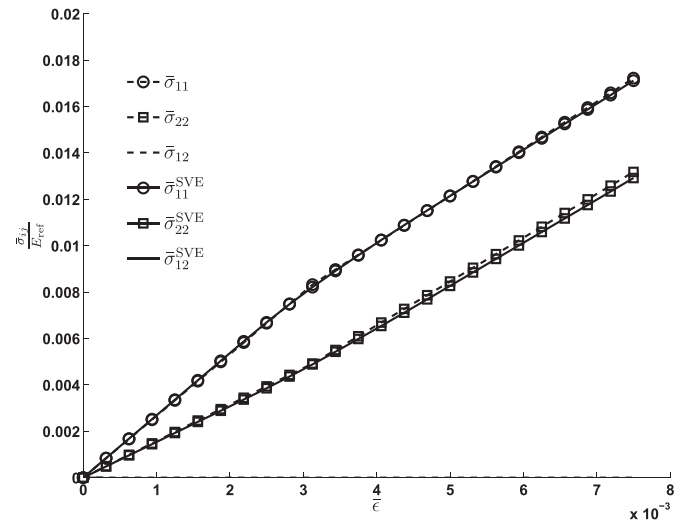

Fig. 14. Convergence of the Neumann–Voigt approximation of the lower bound on the strain energy, $\overline{w}_{\square}^{\text{LB,appr}}$, with SVE-size. Results are shown for a given fixed mesh. $\tilde{\overline{\varepsilon}} = \overline{\varepsilon}e_1 \otimes e_1$ with $\overline{\varepsilon} = 0.005$. All curves show mean values. Actual bounds (Dirichlet–Voigt and Neumann–Reuss samplings) are shown for comparison.
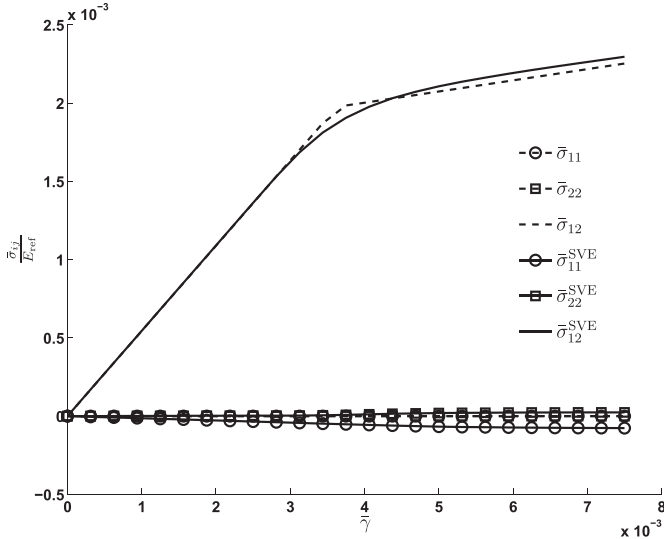
Next, we focus on the effective stress-strain relation and calibrate a macroscopic model of the same form as for the subscale constituents but defined by the parameter set $\pi = \{\overline{E}, \overline{\nu}, \overline{H}, \overline{\sigma}_y\}$. These parameter values are found from a least-squares fit of the corresponding macroscopic (volume-specific) strain energy, denoted $\overline{w}(\pi; \overline{\varepsilon}_i)$, to the mean value of $\overline{w}_{\square}^{\text{UB}}(\overline{\varepsilon}_i)$ and $\overline{w}_{\square}^{\text{LB}}(\overline{\varepsilon}_i)$. Hence, we compute.

$$\underline{\pi} = \arg\min_{\hat{\pi}} \sum_{i}^{M} \frac{1}{2}[\frac{1}{2}[\overline{w}_{\square}^{\text{UB}}(\overline{\varepsilon}_i) + \overline{w}_{\square}^{\text{LB}}(\overline{\varepsilon}_i)] - \overline{w}(\hat{\underline{\pi}}; \overline{\varepsilon}_i)]^2 \tag{138}$$

where M is the number of strain values for which the SVE-problem is analyzed. Here, we use two different types of "virtual tests" for the calibration: macroscopically uniaxial strain, defined by $\overline{\varepsilon} = \overline{\varepsilon}e_1 \otimes e_1$, $0 \leq \overline{\varepsilon} \leq 0.0075$, and macroscopically simple shear, defined by $\overline{\varepsilon} = (1/2)\overline{\gamma}[e_1 \otimes e_2 + e_2 \otimes e_1]$, $0 \leq \overline{\gamma} \leq 0.0075$. In Figs. 15 and 16 the stress–strain response relations for the "upscaled" macroscopic model are compared with those obtained from SVE-computations. In order to facilitate such a comparison, we

Fig. 15. Calibration result: Macroscopic stress–strain relations for uniaxial strain, $\overline{\varepsilon} = \overline{\varepsilon}e_1 \otimes e_1$, $0 \leq \overline{\varepsilon} \leq 0.0075$, whereby $\overline{\varepsilon}$ is the control variable. The figure shows the (smooth) "best fit" of SVE-solutions and the "upscaled" macroscopic (non-smooth) response.

Fig. 16. Calibration result: Macroscopic stress-strain relations for simple shear, $\overline{\varepsilon} = (1/2)\overline{\gamma}[\boldsymbol{e}_1 \otimes \boldsymbol{e}_2 + \boldsymbol{e}_2 \otimes \boldsymbol{e}_1]$, $0 \leq \overline{\gamma} \leq 0.0075$, whereby $\overline{\gamma}$ is the control variable. The figure shows the (smooth) "best fit" of SVE-solutions and the "upscaled" macroscopic (non-smooth) response.

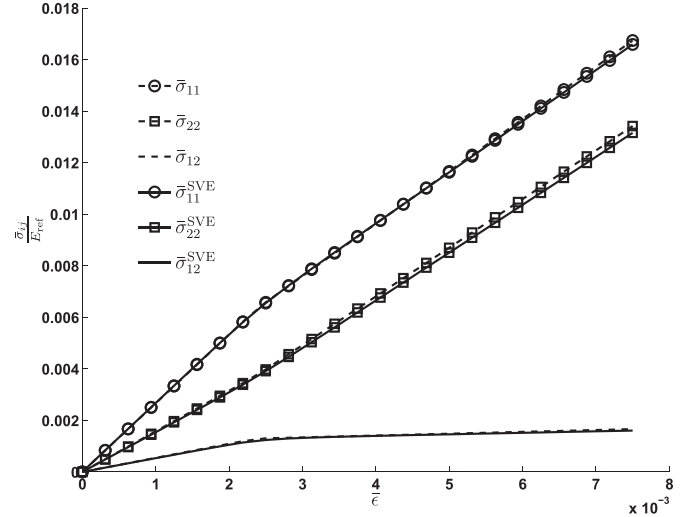**Fig. 17.** Validation result: Macroscopic stress–strain relations for combined uniaxial strain and simple shear. The figure shows the (smooth) "best fit" of SVE-solutions and the "upscaled" macroscopic (non-smooth) response.

identify the particular realization that yields an energy that is closest (in a least squares sense) to the upscaled value, i.e. to the values $(1/2)[\overline{w}_{\square}^{\mathrm{UB}}(\overline{\varepsilon}_i) + \overline{w}_{\square}^{\mathrm{LB}}(\overline{\varepsilon}_i)]$, $i = 1, 2, \ldots, M$, while adopting Dirichlet boundary conditions on SVE. The corresponding stress value from the SVE-computations is denoted $\overline{\sigma}^{\mathrm{SVE}}(\overline{\varepsilon})$. This identification is carried out for a statistical sample consisting of 50 realizations ($N = 50$) for a SVE with fixed size $L_{\square} = 3.75 L_{\mathrm{ref}}$. Obviously, the macroscopic response relations are "non-smooth" by construction, whereas the SVE-results show a smooth transition from the elastic to the elastic–plastic regime. For the simple shear loading in Fig. 16, it is noted that the normal stress in the $\boldsymbol{e}_2$-direction is identically zero for the macroscopic model, whereas a small value is observed for the homogenized response.

Finally, the calibrated macroscopic model is validated for a different loading situation than those used for the calibration, and we choose a combination of the normal and shear strains (still macroscopic strain control): $\overline{\varepsilon} = \overline{\varepsilon}[\boldsymbol{e}_1 \otimes \boldsymbol{e}_1 + (1/2)[\boldsymbol{e}_1 \otimes \boldsymbol{e}_2 + \boldsymbol{e}_2 \otimes \boldsymbol{e}_1]]$, $0 \leq \overline{\varepsilon} \leq 0.0075$. The comparison between the "upscaled" macroscopic model response and the SVE-result is shown in Fig. 17.

6. Conclusions and outlook

In this paper we have presented a computational strategy for obtaining bounds on the effective properties based on homogenization on finite-size SVE:s combined with statistical sampling. Such a strategy has been employed previously in the literature with the more restricted purpose of estimating the effective linear elastic stiffness tensor without confidence intervals on the bounds, e.g. Salmi et al. (2012). The novel feature in this paper is thus that these bounds are computed as strict upper and lower bounds within a given confidence. To compute the upper bound is relatively straightforward, whereas the lower bound represents an additional difficulty. In fact, the theoretically sharpest lower bound (within the given confidence interval) is not feasible in practice due to extensive computational cost; however, it was shown that a slightly less sharp lower bound can be obtained with modest computational effort (defined by the Neumann–Reuss bound and

representing the quasi-optimal choice). Clearly, when the number of realizations for a given SVE-size tends to infinity, then the confidence interval shrinks indefinitely and the bounds become strict.

The "workhorse" for the analysis of a single realization is the weak form of micro-periodicity recently proposed by Larsson et al. (2011). The model setting is that of "incremental elastic energy", which for a dissipative material is obtained by eliminating the internal variables after time integration in a given time step. Hence, for the sake of simplicity it was considered sufficient to consider the generic case of nonlinear elasticity.

As to the future improvements, when assessing the convergence of bounds with increasing SVE-size, it is clear that 3D features of the microstructure should be considered. In addition, it is necessary to include 3D effects in order to make the calibration of an upscaled macroscopic model meaningful in practice.

Future developments include estimation of how subscale FE-discretization error will affect the bounds. In the context of error estimation for the two-scale FE² strategy, it can be established that subscale approximations of different origins appear as model error on the macroscale. However, a distinct difficulty is that it is not possible to establish a hierarchy for the various investigated boundary conditions on the SVE (Dirichlet, weakly periodic and Neumann). Although it turns out that a suitable mix of displacement and traction discretizations in the weak periodicity setting seems to give very accurate answers and rapid convergence to the expected value of the effective properties, it is not possible to establish generally which one of the boundary conditions that is most and least accurate for a given type of micro-heterogeneity and actual macroscale strain field. This issue remains a challenge in, for example, a goal-oriented error computation.

Appendix A. Auxiliary derivations

A.1: Effective strain energy

The SVE-functional (free energy) is defined as $\overline{w}_\square^R$. Since the SVE (a given realization of the micro-heterogeneous material structure) of size $L_\square$ is "loaded" by the given macroscale displacement gradient $\overline{\varepsilon}$, the subscale field $\boldsymbol{u}\{\overline{\varepsilon}\}$ solves the pertinent boundary value problem; hence, $\varepsilon[\boldsymbol{u}] = \varepsilon[\boldsymbol{u}\{\overline{\varepsilon}\}]$. The first and second directional derivatives of $W_\square(\boldsymbol{u})$ are given as.

$$\begin{array}{llll} (W_\square)'(\boldsymbol{u};\delta\boldsymbol{u}) & = & a_\square(\boldsymbol{u};\delta\boldsymbol{u}), & \forall \delta\boldsymbol{u}\in\mathbb{U}_\square \\ (W_\square)''(\boldsymbol{u};\delta\boldsymbol{u}_1,\delta\boldsymbol{u}_2) & = & (a_\square)'(\boldsymbol{u};\delta\boldsymbol{u}_1,\delta\boldsymbol{u}_1), & \forall \delta\boldsymbol{u}_1,\delta\boldsymbol{u}_2\in\mathbb{U}_\square \end{array} \tag{A-1}$$

In order to obtain (A-1)$_1$, we used the relation $\boldsymbol{\sigma} = \mathrm{d}w\{\varepsilon\}/\mathrm{d}\varepsilon$ and the identity $\langle\boldsymbol{\sigma}{:}\varepsilon[\delta\boldsymbol{u}]\rangle_\square = a_\square(\boldsymbol{u};\delta\boldsymbol{u})$.

To show that the solution of the SVE-problem (20), for given $\overline{\varepsilon}$, satisfies the min−max property.

$$(\boldsymbol{u},\boldsymbol{t}) = \arg[\min_{\widehat{\boldsymbol{u}}\in\mathbb{U}_\square} \max_{\widehat{\boldsymbol{t}}\in\mathbb{T}_\square} \Pi_\square(\overline{\varepsilon};\widehat{\boldsymbol{u}},\widehat{\boldsymbol{t}})] \tag{A-2}$$

we consider a stationary point of $\Pi_\square$ defined by the stationary conditions

$$\begin{aligned} (\Pi_\square)'_u(\overline{\varepsilon};\boldsymbol{u},\boldsymbol{t};\delta\boldsymbol{u}) &= (W_\square)'_u(\boldsymbol{u};\delta\boldsymbol{u}) - d_\square(\boldsymbol{t};\delta\boldsymbol{u}) \\ &= a_\square(\boldsymbol{u};\delta\boldsymbol{u}) - d_\square(\boldsymbol{t};\delta\boldsymbol{u}) = 0, \quad \forall\delta\boldsymbol{u}\in\mathbb{U}_\square \\ (\Pi_\square)'_t(\overline{\varepsilon};\boldsymbol{u},\boldsymbol{t};\delta\boldsymbol{t}) &= -d_\square(\delta\boldsymbol{t},\boldsymbol{u}-\overline{\varepsilon}\cdot[\boldsymbol{x}-\overline{\boldsymbol{x}}]) = 0, \quad \forall\delta\boldsymbol{t}\in\mathbb{T}_\square \end{aligned} \tag{A-3}$$

The solution $\boldsymbol{u}\{\overline{\varepsilon}\},\boldsymbol{t}\{\overline{\varepsilon}\}$ of (A-3) is indeed identical to the solution of the SVE-problem (20) for given $\overline{\varepsilon}$. Moreover, from the second derivatives.

$$\begin{aligned} (\Pi_\square)''_{uu}(\overline{\varepsilon};\boldsymbol{u},\boldsymbol{t};\delta\boldsymbol{u}_1,\delta\boldsymbol{u}_2) &= (a_\square)'(\boldsymbol{u};\delta\boldsymbol{u}_1,\delta\boldsymbol{u}_2) = (W_\square)''(\boldsymbol{u};\delta\boldsymbol{u}_1,\delta\boldsymbol{u}_2) \\ (\Pi_\square)''_{ut}(\overline{\varepsilon};\boldsymbol{u},\boldsymbol{t};\delta\boldsymbol{u},\delta\boldsymbol{t}) &= -d_\square(\delta\boldsymbol{t},\delta\boldsymbol{u}) = (\Pi_\square)''_{uu}(\overline{\varepsilon};\boldsymbol{u},\boldsymbol{t};\delta\boldsymbol{t},\delta\boldsymbol{u}) \\ (\Pi_\square)''_{tt}(\overline{\varepsilon};\boldsymbol{u},\boldsymbol{t};\delta\boldsymbol{t}_1,\delta\boldsymbol{t}_2) &= 0 \end{aligned} \tag{A-4}$$

and, since $(W_\square)''(\boldsymbol{u};\delta\boldsymbol{u}_1,\delta\boldsymbol{u}_2) > 0$, we conclude that the solution $\boldsymbol{u}\{\overline{\varepsilon}\},\boldsymbol{t}\{\overline{\varepsilon}\}$ represents a min−max property.

Finally, $\overline{w}_\square\{\overline{\varepsilon}\}$ is a potential for $\overline{\boldsymbol{\sigma}}$ in the classical sense, and the macroscale tangent stiffness is positive definite in the discrete space $\mathbb{R}_{sym}^{3\times3}$, i.e.

$$\overline{\boldsymbol{\sigma}}\{\overline{\varepsilon}\} = \frac{\mathrm{d}\overline{w}_\square\{\overline{\varepsilon}\}}{\mathrm{d}\overline{\varepsilon}}, \quad \overline{\mathbf{E}}_\square\{\overline{\varepsilon}\} \stackrel{\text{def}}{=} \frac{\mathrm{d}^2\overline{w}_\square\{\overline{\varepsilon}\}}{\mathrm{d}\overline{\varepsilon}\otimes\mathrm{d}\overline{\varepsilon}} > 0 \tag{A-5}$$

To show this result, we consider the total differential of $\overline{w}_\square\{\overline{\varepsilon}\}$. Firstly, from the definition of $\overline{w}_\square\{\overline{\varepsilon}\}$ in (34) follows that $\mathrm{d}\overline{w}_\square\{\overline{\varepsilon}\} = (W_\square)'_u(\boldsymbol{u}\{\overline{\varepsilon}\};\mathrm{d}\boldsymbol{u})$. Then, using the relation (A-1)$_1$ with the choice $\delta\boldsymbol{u} = \mathrm{d}\boldsymbol{u}$ and using the variational format (20) or (A-3)$_1$, we obtain.

$$\begin{aligned} \mathrm{d}\overline{w}_\square\{\overline{\varepsilon}\} &= a_\square(\boldsymbol{u}\{\overline{\varepsilon}\};\mathrm{d}\boldsymbol{u}) = d_\square(\boldsymbol{t}\{\overline{\varepsilon}\},\mathrm{d}\boldsymbol{u}) \\ &= d_\square(\boldsymbol{t}\{\overline{\varepsilon}\},\mathrm{d}\overline{\varepsilon}\cdot[\boldsymbol{x}-\overline{\boldsymbol{x}}]) = \sum_{i,j}d_\square(\boldsymbol{t}\{\overline{\varepsilon}\},\widehat{\boldsymbol{u}}^{\mathrm{M}(ij)})\boldsymbol{e}_i\otimes\boldsymbol{e}_j : \mathrm{d}\overline{\varepsilon} \end{aligned} \tag{A-6}$$

However, we also have, by virtue of (20)$_1$,

$$\overline{\boldsymbol{\sigma}}\{\overline{\varepsilon}\} = \sum_{i,j}a_\square(\boldsymbol{u}\{\overline{\varepsilon}\},\widehat{\boldsymbol{u}}^{\mathrm{M}(ij)})\boldsymbol{e}_i\otimes\boldsymbol{e}_j = \sum_{i,j}d_\square(\boldsymbol{t}\{\overline{\varepsilon}\},\widehat{\boldsymbol{u}}^{\mathrm{M}(ij)})\boldsymbol{e}_i\otimes\boldsymbol{e}_j \tag{A-7}$$

Upon combining the results (A-6) and (A-7), we obtain $\mathrm{d}\overline{w}_\square\{\overline{\varepsilon}\} = \overline{\boldsymbol{\sigma}}\{\overline{\varepsilon}\} : \mathrm{d}\overline{\varepsilon}$, which is (A-5)$_1$.

Finally, to show the convexity of $\overline{W}_\square\{\overline{\varepsilon}\}$ in $\mathbb{R}_{sym}^{3\times3}$ we use (A-6), (A-7) and consider the inequality.

$$\begin{aligned} 0 \le (W_\square)''(\boldsymbol{u}\{\overline{\varepsilon}\};\mathrm{d}\boldsymbol{u},\mathrm{d}\boldsymbol{u}) &= \sum_{i,j}d_\square(\mathrm{d}\boldsymbol{t},\widehat{\boldsymbol{u}}^{\mathrm{M}(ij)})\boldsymbol{e}_i\otimes\boldsymbol{e}_j : \mathrm{d}\overline{\varepsilon} = \mathrm{d}\overline{\boldsymbol{\sigma}} : \mathrm{d}\overline{\varepsilon} \\ &= \mathrm{d}\overline{\varepsilon} : \overline{\mathbf{E}}_\square\{\overline{\varepsilon}\} : \mathrm{d}\overline{\varepsilon} \end{aligned} \tag{A-8}$$

to obtain that $\overline{\mathbf{E}}_\square$ is positive definite, i.e. $\overline{w}_\square$ is convex.

A.2: Effective stress energy

We now consider macroscale stress control. To show that the solution of the SVE-problem (27), for given $\overline{\boldsymbol{\sigma}}$, satisfies the max-min-max property.

$$(\boldsymbol{u},\boldsymbol{t},\overline{\varepsilon}) = \arg[\max_{\widehat{\boldsymbol{u}}\in\mathbb{U}_\square} \min_{\widehat{\boldsymbol{t}}\in\mathbb{T}_\square} \max_{\widehat{\overline{\varepsilon}}\in\mathbb{R}_{sym}^{3\times3}} \Pi_\square^*(\overline{\boldsymbol{\sigma}};\widehat{\boldsymbol{u}},\widehat{\boldsymbol{t}},\widehat{\overline{\varepsilon}})] \tag{A-9}$$

we consider a stationary point of $\Pi_\square^*$ defined by the stationary conditions

$$\begin{aligned} (\Pi_\square^*)'_u(\overline{\boldsymbol{\sigma}};\boldsymbol{u},\boldsymbol{t},\overline{\varepsilon};\delta\boldsymbol{u}) &= -(W_\square)'_u(\boldsymbol{u};\delta\boldsymbol{u}) + d_\square(\boldsymbol{t};\delta\boldsymbol{u}) \\ &= -a_\square(\boldsymbol{u};\delta\boldsymbol{u}) + d_\square(\boldsymbol{t};\delta\boldsymbol{u}) = 0, \quad \forall\delta\boldsymbol{u}\in\mathbb{U}_\square \\ (\Pi_\square^*)'_t(\overline{\boldsymbol{\sigma}};\boldsymbol{u},\boldsymbol{t},\overline{\varepsilon};\delta\boldsymbol{t}) &= d_\square(\delta\boldsymbol{t},\boldsymbol{u}-\overline{\varepsilon}\cdot[\boldsymbol{x}-\overline{\boldsymbol{x}}]) = 0, \quad \forall\delta\boldsymbol{t}\in\mathbb{T}_\square \\ (\Pi_\square^*)'_{\overline{\varepsilon}}(\overline{\boldsymbol{\sigma}};\boldsymbol{u},\boldsymbol{t},\overline{\varepsilon};\delta\overline{\varepsilon}) &= \overline{\boldsymbol{\sigma}}:\delta\overline{\varepsilon} - d_\square(\boldsymbol{t},\delta\overline{\varepsilon}\cdot[\boldsymbol{x}-\overline{\boldsymbol{x}}]) = 0, \quad \forall\delta\overline{\varepsilon}\in\mathbb{R}_{sym}^{3\times3} \end{aligned} \tag{A-10}$$

The solution $\boldsymbol{u}\{\overline{\boldsymbol{\sigma}}\},\boldsymbol{t}\{\overline{\boldsymbol{\sigma}}\},\overline{\varepsilon}\{\overline{\boldsymbol{\sigma}}\}$ of (A-10) is indeed identical to the solution of the SVE-problem (27) for given $\overline{\boldsymbol{\sigma}}$.

It also appears that $\overline{w}_\square^*\{\overline{\boldsymbol{\sigma}}\}$ is a potential for $\overline{\varepsilon}$ in the classical sense, and the macroscale tangent compliance is positive definite in the discrete space $\mathbb{R}_{sym}^{3\times3}$, i.e.

$$\overline{\varepsilon}\{\overline{\boldsymbol{\sigma}}\} = \frac{\mathrm{d}\overline{w}_\square^*\{\overline{\boldsymbol{\sigma}}\}}{\mathrm{d}\overline{\boldsymbol{\sigma}}}, \quad \overline{\mathbf{C}}_\square\{\overline{\boldsymbol{\sigma}}\} \stackrel{\text{def}}{=} \frac{\mathrm{d}^2\overline{w}_\square^*\{\overline{\boldsymbol{\sigma}}\}}{\mathrm{d}\overline{\boldsymbol{\sigma}}\otimes\mathrm{d}\overline{\boldsymbol{\sigma}}} > 0 \tag{A-11}$$

To show this result, we consider the total differential of $\overline{w}_\square^*\{\overline{\boldsymbol{\sigma}}\}$. Firstly, from the definition in (38) follows that.

$$\mathrm{d}\overline{w}_\square^*\{\overline{\boldsymbol{\sigma}}\} = \mathrm{d}\overline{\boldsymbol{\sigma}} : \overline{\varepsilon}\{\overline{\boldsymbol{\sigma}}\} + \overline{\boldsymbol{\sigma}} : \mathrm{d}\overline{\varepsilon} - (W_\square)'(\boldsymbol{u}\{\overline{\boldsymbol{\sigma}}\};\mathrm{d}\boldsymbol{u}) \tag{A-12}$$

The last two terms in (A-12) cancel each other, which may be shown as follows: Take the total differential of (A-10)$_2$ to obtain.

$$d_\square(\delta\boldsymbol{t},\mathrm{d}\boldsymbol{u}) - d_\square(\mathrm{d}\overline{\varepsilon}\cdot[\boldsymbol{x}-\overline{\boldsymbol{x}}]) = 0, \quad \forall\delta\boldsymbol{t}\in\mathbb{T}_\square \tag{A-13}$$

Now, setting $\delta\boldsymbol{u} = \mathrm{d}\boldsymbol{u}$ in (A-10)$_1$, $\delta\overline{\varepsilon} = \mathrm{d}\overline{\varepsilon}$ in (A-10)$_3$ and $\delta\boldsymbol{t} = \boldsymbol{t}$ in (A-13) and adding the results to obtain the desired result, we conclude that $\mathrm{d}\overline{w}_\square^*\{\overline{\boldsymbol{\sigma}}\} = \overline{\varepsilon}\{\overline{\boldsymbol{\sigma}}\} : \mathrm{d}\overline{\boldsymbol{\sigma}}$ which is (A-11)$_1$.

In a fashion that is identical to that one used to show convexity of $\overline{w}_\square\{\overline{\varepsilon}\}$, one may show that $\overline{w}_\square^*\{\overline{\boldsymbol{\sigma}}\}$ is convex in the discrete space $\mathbb{R}_{sym}^{3\times3}$. As a preliminary, we take the total differential of (A-10)$_3$ to obtain.

$$\mathrm{d}\overline{\boldsymbol{\sigma}} : \delta\overline{\varepsilon} - d_\square(\mathrm{d}\boldsymbol{t},\delta\overline{\varepsilon}\cdot[\boldsymbol{x}-\overline{\boldsymbol{x}}]) = 0, \quad \forall\delta\overline{\varepsilon}\in\mathbb{R}_{sym}^{3\times3} \tag{A-14}$$

Upon setting $\delta\overline{\varepsilon} = \mathrm{d}\overline{\varepsilon}$ in (A-14) and $\delta\boldsymbol{t} = \mathrm{d}\boldsymbol{t}$ in (A-13) and subtracting the results, we obtain the relation $\mathrm{d}\overline{\boldsymbol{\sigma}} : \mathrm{d}\overline{\varepsilon} = d_\square(\mathrm{d}\boldsymbol{t},\mathrm{d}\boldsymbol{u})$. We are now in the position to consider the inequality.

$$\begin{aligned} 0 \le (W_\square)''(\boldsymbol{u}\{\overline{\boldsymbol{\sigma}}\};\mathrm{d}\boldsymbol{u},\mathrm{d}\boldsymbol{u}) &= (a_\square)'(\boldsymbol{u}\{\overline{\boldsymbol{\sigma}}\};\mathrm{d}\boldsymbol{u},\mathrm{d}\boldsymbol{u}) = d_\square(\mathrm{d}\boldsymbol{t},\mathrm{d}\boldsymbol{u}) \\ &= \mathrm{d}\overline{\boldsymbol{\sigma}} : \mathrm{d}\overline{\varepsilon} = \mathrm{d}\overline{\boldsymbol{\sigma}} : \overline{\mathbf{C}}_\square\{\overline{\boldsymbol{\sigma}}\} : \mathrm{d}\overline{\boldsymbol{\sigma}} \end{aligned} \tag{A-15}$$

to obtain that $\overline{\mathbf{C}}_\square$ is positive definite, i.e. $\overline{w}_\square^*$ is convex.

Remark: We have, in fact, obtained the standard relations between $\overline{w}_\square\{\overline{\boldsymbol{\varepsilon}}\}$ and $\overline{w}_\square^*\{\overline{\boldsymbol{\sigma}}\}$:

$$\overline{w}_\square^*\{\overline{\boldsymbol{\sigma}}\} = \max_{\widehat{\overline{\boldsymbol{\varepsilon}}}\in\mathbb{R}_{\text{sym}}^{3\times3}} [\overline{\boldsymbol{\sigma}} : \widehat{\overline{\boldsymbol{\varepsilon}}} - \overline{w}_\square\{\widehat{\overline{\boldsymbol{\varepsilon}}}\}] \qquad (A\text{-}16)$$

$$\overline{w}_\square\{\overline{\boldsymbol{\varepsilon}}\} = \max_{\widehat{\overline{\boldsymbol{\sigma}}}\in\mathbb{R}_{\text{sym}}^{3\times3}} [\widehat{\overline{\boldsymbol{\sigma}}} : \overline{\boldsymbol{\varepsilon}} - \overline{w}_\square^*\{\widehat{\overline{\boldsymbol{\sigma}}}\}] \qquad (A\text{-}17)$$

which are classical Legendre transformations.

A.3: Guaranteed upper bound on effective strain energy

Recalling the definition of $\overline{w}_\square\{\overline{\boldsymbol{\varepsilon}}\}$ in (A-2), we have for the "super-SVE"

$$\overline{w}_{(\square)}\{\overline{\boldsymbol{\varepsilon}}\} = \min_{\widehat{\boldsymbol{u}}\in\mathbb{U}_{(\square)}} \max_{\widehat{\boldsymbol{t}}\in\mathbb{T}_{(\square)}} \Pi_{(\square)}(\overline{\boldsymbol{\varepsilon}};\widehat{\boldsymbol{u}},\widehat{\boldsymbol{t}}) \qquad (A\text{-}18)$$

with the obvious definition of the HR-potential $\Pi_{(\square)}$, cf. the expression for $\Pi_\square(\overline{\boldsymbol{\varepsilon}};\widehat{\boldsymbol{u}},\widehat{\boldsymbol{t}})$ in (33), and the spaces $\mathbb{U}_{(\square)}$ and $\mathbb{T}_{(\square)}$. Since $\mathbb{U}_{(\square)}^D\subseteq\mathbb{U}_{(\square)}$, we have

$$\overline{w}_{(\square)}\{\overline{\boldsymbol{\varepsilon}}\} \leq \min_{\widehat{\boldsymbol{u}}\in\mathbb{U}_{(\square)}^D} \max_{\widehat{\boldsymbol{t}}\in\mathbb{T}_{(\square)}} \Pi_{(\square)}(\overline{\boldsymbol{\varepsilon}};\widehat{\boldsymbol{u}},\widehat{\boldsymbol{t}}) \qquad (A\text{-}19)$$

Now, we introduce the restricted displacement space $\overline{\mathbb{U}}_{(\square)}^D\subseteq\mathbb{U}_{(\square)}^D$, defined as.

$$\overline{\mathbb{U}}_{(\square)}^D = \{\widehat{\boldsymbol{u}}\in\mathbb{U}_{(\square)}^D(\overline{\boldsymbol{\varepsilon}}) : \widehat{\boldsymbol{u}} = \overline{\boldsymbol{\varepsilon}}\cdot[\boldsymbol{x}-\overline{\boldsymbol{x}}] \text{ on each } \Gamma_{\square,i}\} \qquad (A\text{-}20)$$

The displacements in this space thus obey the "Taylor assumption" in a restricted sense on all the SVE-boundaries inside the super-SVE. We thus obtain.

$$\overline{w}_{(\square)}\{\overline{\boldsymbol{\varepsilon}}\} \leq \min_{\widehat{\boldsymbol{u}}\in\overline{\mathbb{U}}_{(\square)}^D} \max_{\widehat{\boldsymbol{t}}\in\mathbb{T}_{(\square)}} \Pi_{(\square)}(\overline{\boldsymbol{\varepsilon}};\widehat{\boldsymbol{u}},\widehat{\boldsymbol{t}})$$
$$= \frac{1}{N}\sum_{j=1}^N \min_{\widehat{\boldsymbol{u}}\in\mathbb{U}_{\square,j}^D} \max_{\widehat{\boldsymbol{t}}\in\mathbb{T}_{\square,j}} \Pi_{\square,j}(\overline{\boldsymbol{\varepsilon}};\widehat{\boldsymbol{u}},\widehat{\boldsymbol{t}}) = \frac{1}{N}\sum_{j=1}^N \overline{w}_{\square,j}^D\{\overline{\boldsymbol{\varepsilon}}\} \qquad (A\text{-}21)$$

Since $L_{(\square)}\to\infty$ corresponds to $N\to\infty$, the result in (52) follows.

A.4: Guaranteed upper bound on effective stress energy

Recalling the definition of $\overline{w}_\square^*\{\overline{\boldsymbol{\sigma}}\}$ in (A-9), we have for the "super-SVE"

$$\overline{w}_{(\square)}^*\{\overline{\boldsymbol{\sigma}}\} = \max_{\widehat{\boldsymbol{u}}\in\mathbb{U}_{(\square)}} \min_{\widehat{\boldsymbol{t}}\in\mathbb{T}_{(\square)}} \max_{\widehat{\overline{\boldsymbol{\varepsilon}}}\in\mathbb{R}_{\text{sym}}^{3\times3}} \Pi_{(\square)}^*(\overline{\boldsymbol{\sigma}};\widehat{\boldsymbol{u}},\widehat{\boldsymbol{t}},\widehat{\overline{\boldsymbol{\varepsilon}}}) \qquad (A\text{-}22)$$

Since $\mathbb{T}_{(\square)}^N\subseteq\mathbb{T}_{(\square)}$, we have.

$$\overline{w}_{(\square)}^*\{\overline{\boldsymbol{\sigma}}\} \leq \max_{\widehat{\boldsymbol{u}}\in\mathbb{U}_{(\square)}} \min_{\widehat{\boldsymbol{t}}\in\mathbb{T}_{(\square)}^N} \max_{\widehat{\overline{\boldsymbol{\varepsilon}}}\in\mathbb{R}_{\text{sym}}^{3\times3}} \Pi_{(\square)}^*(\overline{\boldsymbol{\sigma}};\widehat{\boldsymbol{u}},\widehat{\boldsymbol{t}},\widehat{\overline{\boldsymbol{\varepsilon}}}) \qquad (A\text{-}23)$$

Now, we relax the continuity of displacements between each SVE occupying the domain $\Omega_{\square,i}$ by introducing the "broken space" of displacements for the super-SVE and the corresponding space of tractions:

$$\overline{\mathbb{U}}_{(\square)} = \{\widehat{\boldsymbol{u}} \text{ sufficiently regular in each } \Omega_{\square,i},\ i=1,...,N\} \qquad (A\text{-}24)$$

$$\overline{\mathbb{T}}_{(\square)}^N = \{\widehat{\boldsymbol{t}}\in\mathbb{T}_{(\square)}^N \Big| \widehat{\boldsymbol{t}} = \widehat{\overline{\boldsymbol{\sigma}}}\cdot\boldsymbol{n} \text{ on each } \Gamma_{\square,i}^+,\ i=1,...,N\} \qquad (A\text{-}25)$$

The displacements in $\overline{\mathbb{U}}_{(\square)}$ may thus be discontinuous across the SVE-boundaries inside the super-SVE, and we denote the (possible) jump by $[\![\boldsymbol{u}]\!]$. As to the definition of the traction space $\overline{\mathbb{T}}_{(\square)}^N$, we introduced the normal $\boldsymbol{n}$ on each positive boundary $\Gamma_{\square,i}^+$. Clearly the tractions represent Neumann conditions on each $\Omega_{\square,i}$ (and not only on the boundary of the super-SVE); hence, $\overline{\mathbb{T}}_{(\square)}^N\subseteq\mathbb{T}_{(\square)}^N$.

Upon introducing the notion $\Gamma_{\text{int}} = \cup_i\Gamma_{\square,i}\backslash\Gamma_{(\square)}$ for the union of internal boundaries, we are in the position to replace the inequality in (A-23) by.

$$\overline{w}_{(\square)}^*\{\overline{\boldsymbol{\sigma}}\} \leq \max_{\widehat{\boldsymbol{u}}\in\overline{\mathbb{U}}_{(\square)}} \min_{\widehat{\boldsymbol{t}}\in\overline{\mathbb{T}}_{(\square)}^N} \max_{\widehat{\overline{\boldsymbol{\varepsilon}}}\in\mathbb{R}_{\text{sym}}^{3\times3}} \overline{\Pi}_{(\square)}^*(\overline{\boldsymbol{\sigma}};\widehat{\boldsymbol{u}},\widehat{\boldsymbol{t}},\widehat{\overline{\boldsymbol{\varepsilon}}}) \qquad (A\text{-}26)$$

where we introduced the "relaxed" functional

$$\overline{\Pi}_{(\square)}^*(\overline{\boldsymbol{\sigma}};\widehat{\boldsymbol{u}},\widehat{\boldsymbol{t}},\widehat{\overline{\boldsymbol{\varepsilon}}})\stackrel{\text{def}}{=}\Pi_{(\square)}^*(\overline{\boldsymbol{\sigma}};\widehat{\boldsymbol{u}},\widehat{\boldsymbol{t}},\widehat{\overline{\boldsymbol{\varepsilon}}}) + \frac{1}{|\Omega_{(\square)}|}\int_{\Gamma_{\text{int}}} \widehat{\boldsymbol{t}}\cdot[\![\widehat{\boldsymbol{u}}]\!]\,\text{dS}$$

$$(A\text{-}27)$$

Upon using the explicit expression of $\Pi_{(\square)}^*(\overline{\boldsymbol{\sigma}};\widehat{\boldsymbol{u}},\widehat{\boldsymbol{t}},\widehat{\overline{\boldsymbol{\varepsilon}}})$, cf. the expression for $\Pi_\square^*(\overline{\boldsymbol{\sigma}};\widehat{\boldsymbol{u}},\widehat{\boldsymbol{t}},\widehat{\overline{\boldsymbol{\varepsilon}}})$ in (37), and the specific properties of $\overline{\mathbb{T}}_{(\square)}^N$, we may reformulate (A-26) as.

$$\overline{w}_{(\square)}^*\{\overline{\boldsymbol{\sigma}}\} \leq \max_{\widehat{\overline{\boldsymbol{\varepsilon}}}\in\mathbb{R}_{\text{sym}}^{3\times3}} \min_{\widehat{\overline{\boldsymbol{\sigma}}}\in\mathbb{R}_{\text{sym}}^{3\times3}} \max_{\widehat{\boldsymbol{u}}\in\overline{\mathbb{U}}_{(\square)}} \left[[\overline{\boldsymbol{\sigma}}-\widehat{\overline{\boldsymbol{\sigma}}}] : \widehat{\overline{\boldsymbol{\varepsilon}}} + \frac{1}{N}\sum_{i=1}^N [\widehat{\overline{\boldsymbol{\sigma}}} \right.$$
$$\left. : \langle\boldsymbol{\varepsilon}[\widehat{\boldsymbol{u}}]\rangle_{\square,i}-W_{\square,i}(\widehat{\boldsymbol{u}})]\right] = \frac{1}{N}\sum_{i=1}^N \max_{\widehat{\boldsymbol{u}}\in\overline{\mathbb{U}}_{\square,i}} [\overline{\boldsymbol{\sigma}}$$
$$: \langle\boldsymbol{\varepsilon}[\widehat{\boldsymbol{u}}]\rangle_{\square,i}-W_{\square,i}(\widehat{\boldsymbol{u}})] = \frac{1}{N}\sum_{i=1}^N \overline{w}_{\square,i}^{*N}\{\overline{\boldsymbol{\sigma}}\}$$

$$(A\text{-}28)$$

Again, since $L_{(\square)}\to\infty$ corresponds to $N\to\infty$, the result in (54) follows.

References

Brisard, S., Sab, K., Dormieux, L., 2013. New boundary conditions for the computation of the apparent stiffness of statistical volume elements. J. Mech. Phys. Solids 61 (12), 2638–2658.

Danielsson, M., Parks, D.M., Boyce, M.C., 2007. Micromechanics, macromechanics and constitutive modeling of the elasto-viscoplastic deformation of rubber-toughened glassy polymers. J. Mech. Phys. Solids 55 (3), 533–561.

Geers, M.G.D., Kouznetsova, V.G., Brekelmans, W.A.M., 2010. Multi-scale computational homogenization: trends and challenges. J. Comput. Appl. Math. 234, 2175–2182.

Hazanov, S., Huet, C., 1995. Order relationships for boundary condition effects in heterogeneous bodies smaller than the representative volume. J. Mech. Phys. Solids 42, 1995–2011.

Huet, C., 1990. Application of variational concepts to size effects in elastic heterogeneous bodies. J. Mech. Phys. Solids 38, 813–841.

Kouznetsova, V., Geers, M.G.D., Brekelmans, W.A.M., 2002. Multi-scale constitutive modelling of heterogeneous materials with a gradient-enhanced computational homogenization scheme. Int. J. Numer. Methods Eng. 54, 1235–1260.

Larsson, F., Runesson, K., Saroukhani, S., Vafadari, R., 2011. Computational homogenization based on a weak format of micro-periodicity for RVE-problems. Comput. Methods Appl. Mech. Eng. 200, 11–26.

Larsson, F., Runesson, K., Su, F., 2010. Variationally consistent computational homogenization of transient heat flow. Int. J. Numer. Methods Eng. 81, 1659–1686.

Michel, J.C., Moulinec, H., Suquet, P., 1999. Effective properties of composite materials with periodic microstructure: a computational approach. Comput. Methods Appl. Mech. Eng. 172, 109–143.

Miehe, C., Koch, A., 2002. Computational micro-to-macro transitions of discretized microstructures undergoing small strains. Arch. Appl. Mech. 72, 300–317.

Miehe, C., Schröder, J., Schotte, J., 1999. Computational homogenization analysis in finite plasticity simulation of texture development in polycrystalline materials. Comput. Methods Appl. Mech. Eng. 171, 387–418.

Nguyen, Q.-S., 2010. On standard dissipative gradient models. Ann. Solid Struct. Mech. 1, 79–86.

Ostoja-Starzewski, M., 2006. Material spatial randomness: from statistical to representative volume element. Probab. Eng. Mech. 21, 112–132.

Ostoja-Starzewski, M., 2008. Microstructural Randomness and Scaling in Mechanics of Materials. Chapman & Hall/CRC Taylor & Francis Group.

Quilici, S., Cailletaud, G., 1999. FE simulation of macro-, meso-, and microscales in polycristaline plasticity. Comput. Mater. Sci. 16, 383–390.

Roters, F., Eisenlohr, P., Hantcherli, L., Tjahjanto, D.D., Bieler, T.R., Raabe, D., 2010. Overview of constitutive laws, kinematics, homogenization and multiscale methods in crystal plasticity finite-element modeling: theory, experiments, applications. Acta Mater. 58, 1152–1211.

Salmi, M., Auslender, F., Bornert, M., Fogli, M., 2012. Apparent and effective mechanical properties of linear matrix-inclusion random composites: improved bounds for the effective behavior. Int. J. Solids Struct. 49 (10), 1195–1211.

Schmauder, S., Wulf, J., Steinkopff, T., Fischmeister, H., 1996. Micromechanics of plasticity and damage in an al/sic metal matrix composite. In: Pineau, A., Zaoui, A. (Eds.), Micromechanics of Elasticity and Damage of Multiphase Materials. Kluwer Academic Publishers.

Schröder, J., Balzani, D., Brands, D., 2011. Approximation of random microstructures by periodic statistically similar representative volume elements based on lineal-path functions. Arch. Appl. Mech. 81, 975–997.

Suquet, P.M., 1977. Effective properties of nonlinear composites. In: Suquet, P.M. (Ed.), Continuum Micromechanics, CISM Courses and Lectures, Udine. Springer Verlag, Berlin, pp. 197–264.

Suquet, P.M., 1993. Overall potentials and extremal surfaces of power law or ideally plastic materials. J. Mech. Phys. Solids 41, 981–1002.

Temizer, I., Wriggers, P., 2008. On the computation of the macroscopic tangent for multiscale volumetric homogenization problems. Comput. Methods Appl. Mech. Eng. 198, 495–510.

Teply, J.L., Dvorak, G., 1988. Bounds on overall instantaneous properties of elastic-plastic composites. J. Mech. Phys. Solids 36, 29–58.

Torquato, S., 2002. Random Heterogeneous Materials. Microstructure and Macroscopic Properties. Springer Verlag.

Zohdi, T., Wriggers, P., 2001. A model for simulating the deterioration of structural-scale material responses of microheterogeneous solids. Comput. Methods Appl. Mech. Eng. 190, 2803–2823.

Zohdi, T.I., Wriggers, P., 2005. Introduction to Computational Micromechanics. Springer.